Functional Evaluation of the Heart by Transesophageal Echocardiography

5

Benjamin W. Eidem

Abstract

The noninvasive echocardiographic evaluation of ventricular performance is an essential tool in the clinician's assessment and management of children and adults with congenital heart disease (CHD). However the unique anatomic and physiologic features in these patients, which include nonstandard ventricular geometries as well as variable loading conditions, can make the quantitative assessment of ventricular function challenging, particularly by transesophageal echocardiography (TEE). Newer echocardiographic methods are enabling more accurate and quantitative evaluation of ventricular performance, both by the transthoracic as well as the transesophageal approach. This chapter discusses the current applications of TEE in the evaluation of ventricular function in patients with CHD.

Introduction

The noninvasive echocardiographic evaluation of ventricular performance is an essential tool in the clinician's assessment and management of children and adults with congenital heart disease (CHD). As noninvasive methods have continued to evolve, the importance of global and regional ventricular function has become better appreciated. Alterations in both ventricular geometry and loading conditions are the hallmarks of many congenital heart lesions and can make the quantitative assessment of ventricular function challenging. While transesophageal echocardiography (TEE) has often historically been limited to a subjective assessment of ventricular function, newer echocardiographic methods allow more accurate and quantitative evaluation of ventricular performance by the transesophageal approach. This chapter focuses on the current applications of TEE in the evaluation of ventricular function in patients with CHD. Many of these concepts are also relevant to the assessment of ventricular function in children with acquired cardiovascular pathologies.

Transesophageal Echocardiographic Evaluation of Ventricular Function in Congenital Heart Disease

Indications

The majority of patients with CHD have excellent transthoracic echocardiographic (TTE) windows. However, TEE imaging is particularly helpful in those with challenging surface images, such as adults with CHD or postoperative

B.W. Eidem, MD, FACC, FAAP, FASE
Division of Pediatric Cardiology and Cardiovascular Diseases, Departments of Pediatrics and Medicine, Mayo Clinic, 200 First Street SW, Rochester, MN 55905, USA
e-mail: eidem.benjamin@mayo.edu

patients (Table 5.1). In addition, evaluation of ventricular function in the operating room [1–9] or during interventional cardiac catheterization procedures [10–13], is often best facilitated with TEE imaging.

Imaging Planes

Optimal imaging of the left ventricle (LV) is best achieved with a combination of the transgastric mid left ventricular short axis (TG Mid SAX), transgastric long axis (TG LAX), mid esophageal four chamber (ME 4 Ch), and mid esophageal two chamber (ME 2 Ch) views [14, 15]. The miniaturization of multiplane TEE probes allows for additional imaging planes that are also quite helpful in facilitating better endocardial border definition and optimizing Doppler alignment, particularly in patients with CHD-associated with altered ventricular anatomy and geometry.

Table 5.1 Specific indications for TEE assessment of ventricular function

| |
|---|
| *Limited transthoracic image quality* |
| *Intra-operative assessment of ventricular function* |
| Pre and postoperative assessment of ventricular performance |
| Identification of regional wall motion abnormalities suggesting ischemia |
| Ongoing postoperative assessment of response to medical or surgical or intervention |
| *Evaluation of ventricular function in the critical care setting* |
| Evaluation of unstable hemodynamics |
| Assessment of the integrity of the cardiac repair and its impact on ventricular function |
| Weaning from mechanical circulatory support |
| *Evaluation of ventricular function during interventional cardiac catheterization procedures* |
| Impact of procedure on ventricular performance |

The TG Mid SAX, obtained at the mid papillary level, is the TTE equivalent of the parasternal short axis scan plane and readily facilitates the evaluation of radial ventricular function including LV shortening fraction (Fig. 5.1). This view is also optimal to evaluate regional wall motion abnormalities as all major coronary artery distributions are represented in this view.

The TG LAX view best visualizes the apex of the LV and is also helpful to assess regional wall motion. This plane, in addition to the deep transgastric long axis (DTG LAX) and sagittal (DTG Sagittal) views, allow for optimal spectral Doppler alignment with the left ventricular outflow tract, making quantitative assessment of LV cardiac output feasible.

The ME 4 Ch and ME 2 Ch views are easily obtained from the mid esophageal window. The ME 4 Ch view is most commonly used for simultaneous qualitative assessment of right ventricular (RV) and LV performance (Fig. 5.2a, b). In addition, longitudinal ventricular function is best evaluated in this view due to the optimal alignment with both lateral RV and LV walls. Overall assessment of volume status is also readily appreciated in this four chamber orientation. The ME 2 Ch view provides for biplane measurement of ventricular volume and LV ejection fraction (Fig. 5.2c, d, e).

## Echocardiographic Assessment of Global Left Ventricular Systolic Function

Echocardiographic measures of LV systolic function include M-mode, two-dimensional (2D), three-dimensional (3D), and Doppler-derived indices of ventricular performance. Each of these measures can be readily obtained with TEE [17–42]. The majority of echocardiographic measures of LV systolic function represent ejection phase indices that rely
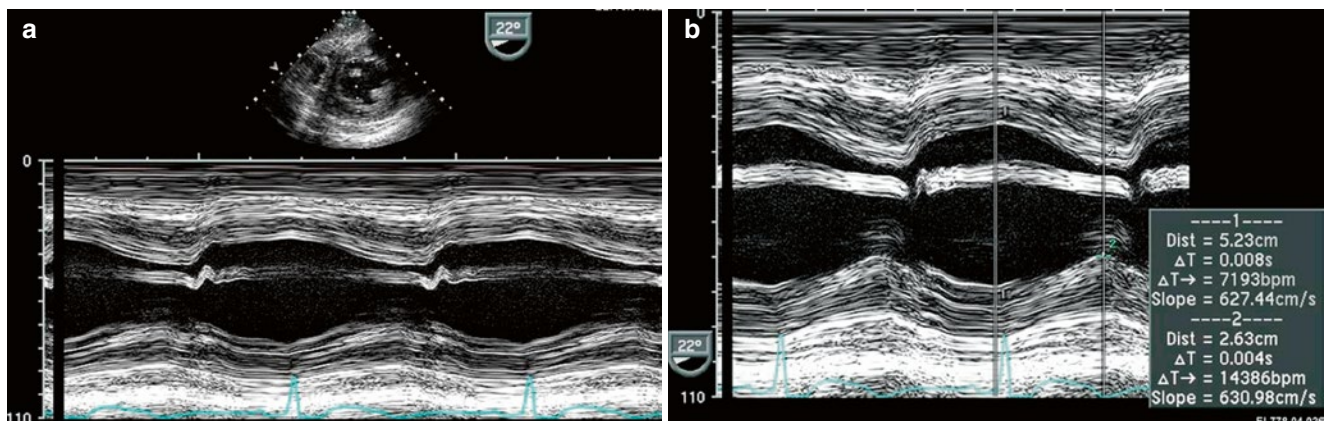
Fig. 5.1 Left ventricular shortening fraction. Transgastric mid short axis image at level of papillary muscles of the left ventricle (LV). (**a**) M-mode demonstrating left ventricular shortening. (**b**) M-mode derived shortening fraction (SF) of the LV:

$$\text{SF }\% = [\text{LVEDD} - \text{LVESD}] / \text{LVEDD}$$
$$= [52 \text{ mm} - 26 \text{ mm}] / 53 \text{ mm} = 50\%$$

LVEDD LV end-diastolic dimension, *LVESD* LV end-systolic dimension

Left ventricular volumes
Method of discs (Simpson's rule)

$$V = \frac{\pi}{4} \sum_{i=1}^{n} a_i b_i \frac{L}{n}$$
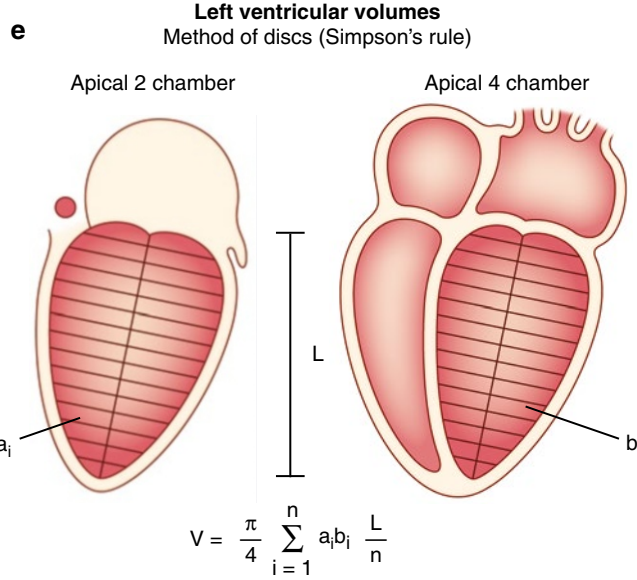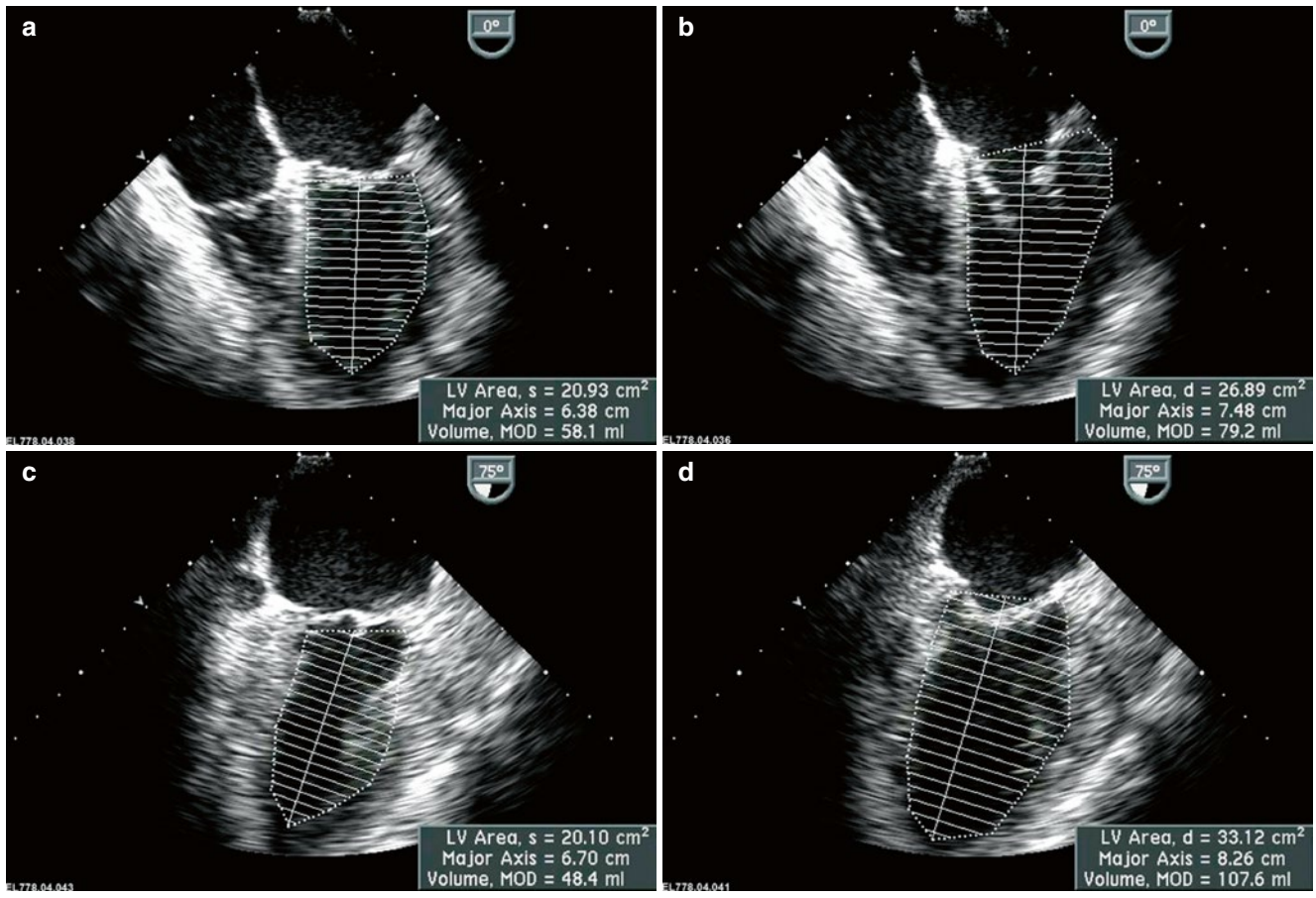
Fig. 5.2 Left ventricular ejection fraction. Four chamber (**a**, **b**) and two chamber (**c**, **d**) views at the level of the mid esophagus in systole (**a**, **c**) and diastole (**b**, **d**). These imaging planes allow quantitative assessment of left ventricular (*LV*) systolic function. Simpson's biplane methodology to calculate LV ejection fraction (**e**), figure adapted from Schiller et al. [16], with permission)

upon geometric assumptions inherent in the elliptical shape of the LV. More importantly, these measurements are significantly influenced by a variety of hemodynamic factors including altered ventricular preload and afterload, heart rate, LV mass, and myocardial contractility. The emergence of Doppler-derived measures of ventricular function has circumvented many of the geometric challenges inherent in this global assessment of ventricular performance. This is

especially the case in the evaluation of RV performance as well as quantitative assessment of systolic function in patients with complex ventricular morphologies. Many of these techniques have been applied using TEE [43–51].

Left Ventricular Shortening Fraction and Fractional Area Change

One-dimensional wall motion analysis, or M-mode echocardiography, has traditionally been one of the most commonly utilized methods to measure the extent of LV shortening. Shortening fraction (SF) represents the change in LV short axis diameter that occurs during systole (Fig. 5.1):

$$LVSF(\%) = [LVEDD - LVESD] / LVEDD \times 100$$

LVEDD = LV end-diastolic dimension; LVESD = LV end-systolic dimension

Normal values for shortening fraction range between 28 and 44 %. The LV TG Mid SAX plane is the TEE view most frequently used to make these measurements. Similar to fractional shortening, fractional area change (FAC) can also be measured in this view by determining the change in LV area that occurs during the cardiac cycle:

$$FAC = [(LV \ end\text{-}diastolic \ area) - (LV \ end\text{-}systolic \ area)] / (LV \ end\text{-}diastolic \ area)$$

Normal values have been reported to be >36 % for fractional area change in adults. LVSF and FAC have been reported to be independent of changes in heart rate and age but are significantly impacted by changes in ventricular preload and afterload [52–56].

A concern regarding this evaluation was raised in a retrospective blinded analysis comparing TTE from TEE-derived FAC measured from LV TG Mid SAX images in pediatric patients with CHD [57]. Potential errors in this measurement were reported as well as significant interobserver variability. In spite of these findings the authors were not able to exclude echocardiographic experience and training of the investigators as potential factors accounting for the variability observed. In this study, TEE-derived FAC measurement was not possible in a significant number of patients due to inability to trace endocardial borders at end-systole. Technological advances since the publication of this work may facilitate this assessment in the current era.

Left Ventricular Ejection Fraction

Left ventricular ejection fraction (LVEF) is the most commonly measured parameter of ventricular systolic function. Global estimation of LVEF is often determined in a qualitative fashion; however, utilizing TTE or TEE, 2D imaging allows quantitative measurement of LVEF by assessing changes in ventricular volume during the cardiac cycle. The geometric model most commonly used for this measurement is the modified Simpson's biplane method (Fig. 5.2e) [16, 58–60]. By utilizing orthogonal four chamber and two chamber views of the LV (from an apical window during TTE), this geometric model calculates LV end-diastolic volume (LVEDV) and LV end-systolic volume (LVESV) by summing equal sequential slices of LV area from each of these scan planes. LVEF can then be calculated as:

$$LVEF (\%) = [LVEDV - LVESV] / LVEDV \times 100$$

Normal values for LVEF range between 56 and 78 %. Similar to LVSF, LVEF has been shown to be dependent on changes in ventricular loading conditions [52, 54–56, 61].

Accurate calculation of LV volume by TEE can be challenging due to foreshortening of the LV cavity. To circumvent this limitation, an area-length method to derive LVEF can also be used [24]. This method utilizes the short axis area of the LV and the long axis LV length and can be obtained by imaging the LV in the TG mid SAX and ME 4 Ch views. Determination of ventricular volume and EF by these TEE methods has been shown to correlate reasonably well with invasively measured parameters of ventricular function.

New echocardiographic technology and advancements in image processing have allowed improved acquisition of ventricular volumes. Studies have validated the ability of 3D echocardiography to obtain accurate and reproducible estimates of LV and RV volumes and EF [32–35, 62–64]. While initially limited by the time-consuming reconstruction of acquired images, advances in 3D TEE now allow for real time data display, significantly enhancing the quantitative assessment of ventricular volume and function (Chap. 19) [63, 65, 66].

Automated border detection (ABD) is another approach in imaging technology that utilizes acoustic quantification to differentiate the myocardium from the blood pool and thereby allows enhanced visualization of the endocardial border. End-diastolic and end-systolic LV area can be continuously displayed with this modality enabling determination of ventricular volume, FAC, and even pressure-volume or pressure-area loops. Excellent correlation of ABD with other noninvasive and invasive measurements of ventricular function has been reported in a few adult studies but data is lacking in patients with CHD and altered ventricular geometry [44, 46, 67–73].

Velocity of Circumferential Fiber Shortening and the Stress–Velocity Index

The rate of LV fiber shortening can be noninvasively assessed by M-mode echocardiography (a graphic display of distance

over time). This measurement, termed the mean velocity of circumferential fiber shortening (V_{cf}), is normalized for LV end-diastolic dimension and can be obtained from the following equation:

$$V_{cf} = [LVEDD - LVESD]/[LVEDD \times LVET]$$

LVET = LV ejection time.

Reported normal values for mean V_{cf} are 1.5 ± 0.04 circumferences (circ)/sec (s) for neonates and 1.3 ± 0.03 circ/s for children between 2 and 10 years of age [54, 74, 75]. This index not only assesses the degree of fractional shortening but the rate at which this shortening occurs. To normalize V_{cf} for variation in heart rate, LVET is divided by the square root of the R-R interval to derive a rate-corrected mean velocity of circumferential fiber shortening (V_{cfc}). Normal V_{cfc} has been reported to be 1.28 ± 0.22 and 1.08 ± 0.14 circ/s in neonates and children, respectively [54, 74–79]. Because V_{cfc} values are corrected for heart rate, a significant decrease in V_{cfc} between the neonatal and childhood age groups has been attributed to increased systemic afterload with advancing age. V_{cf} is sensitive to changes in contractility and afterload but relatively insensitive to changes in preload. Similar to fractional shortening, this parameter relies on the elliptical shape of the LV and is invalid with altered LV geometry.

Because the majority of ejection phase indices, including SF, EF, and V_{cfc} are dependent upon the underlying loading state of the LV, measures of wall tension, namely circumferential and meridional end-systolic wall stress, have been proposed to assess myocardial systolic performance in a relatively load-independent fashion [80]. Colan and colleagues have previously described a stress-velocity index that is an inverse linear relationship between V_{cfc} and end-systolic wall stress (Fig. 5.3). This stress-velocity index is independent of preload, normalized for heart rate, and incorporates afterload resulting in a noninvasive measure of LV contractility that is independent of ventricular loading conditions [81]. This index can therefore provide a more accurate characterization of LV myocardial systolic performance, by differentiating states of increased ventricular afterload from decreased myocardial contractility. While both conditions can affect cardiac output, the former represents increased resistance to myocardial output despite normal myocardial contractility, while the latter represents a true impairment of myocardial contractile performance. While the stress-velocity index is appealing, the clinical application of this index has been limited by its cumbersome acquisition and the need for time-consuming offline processing which are often not suitable for rapid assessment of ventricular performance such as is typically required during TEE. This index is also limited in patients with altered ventricular geometry and wall thickness, features that are hallmarks of CHD.
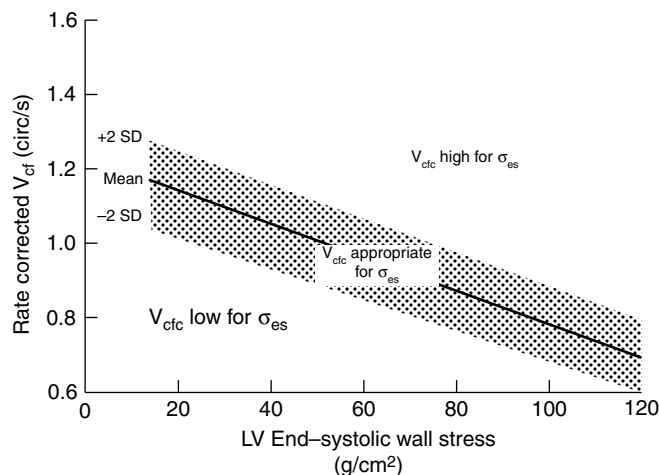

Fig. 5.3 Stress–velocity index for assessment of left ventricular systolic function. Graphic representation of the relationship between the mean rate-corrected velocity of circumferential left ventricular (*LV*) fiber shortening (V_{cfc}) and the LV end-systolic wall stress (σ_{es}). To normalize V_{cf} for variation in heart rate, it is divided by the square root of the R–R interval to derive a rate-corrected mean velocity of circumferential LV fiber shortening (V_{cfc}). Values above the upper limit of the mean relationship imply an increased inotropic state while values below the mean imply depressed contractility (From Colan et al. [81], with permission)

Doppler Parameters of Global Left Ventricular Systolic Function

Echocardiographic evaluation of systolic function has primarily relied upon one-dimensional measures of LV shortening or on 2D measures of LV volume changes that are often difficult to assess in patients with distorted ventricular geometry. Doppler measures of global ventricular function have been reported to be a potentially more reproducible and sensitive measure of ventricular function overcoming the limitations of other approaches.

Left Ventricular dP/dt

Doppler echocardiography can be utilized in the quantitative evaluation of LV systolic function. If mitral regurgitation (MR) is present, the peak and mean rate of change in LV systolic pressure (dP/dt) can be derived from the ascending portion of the continuous wave MR Doppler signal. This rate of change of ventricular pressure is determined during the isovolumic phase of the cardiac cycle before opening of the aortic valve. Utilizing the simplified Bernoulli equation, two velocity points along the MR Doppler envelope are selected from which a corresponding LV pressure change can be derived (Fig. 5.4). This change in LV pressure can then be divided by the change in time between the two Doppler velocities to derive the LV dP/dt. Normal values for mean dP/dt have been reported to be >1,200 mmHg/s for the LV. While more time consuming to perform, peak dP/dt
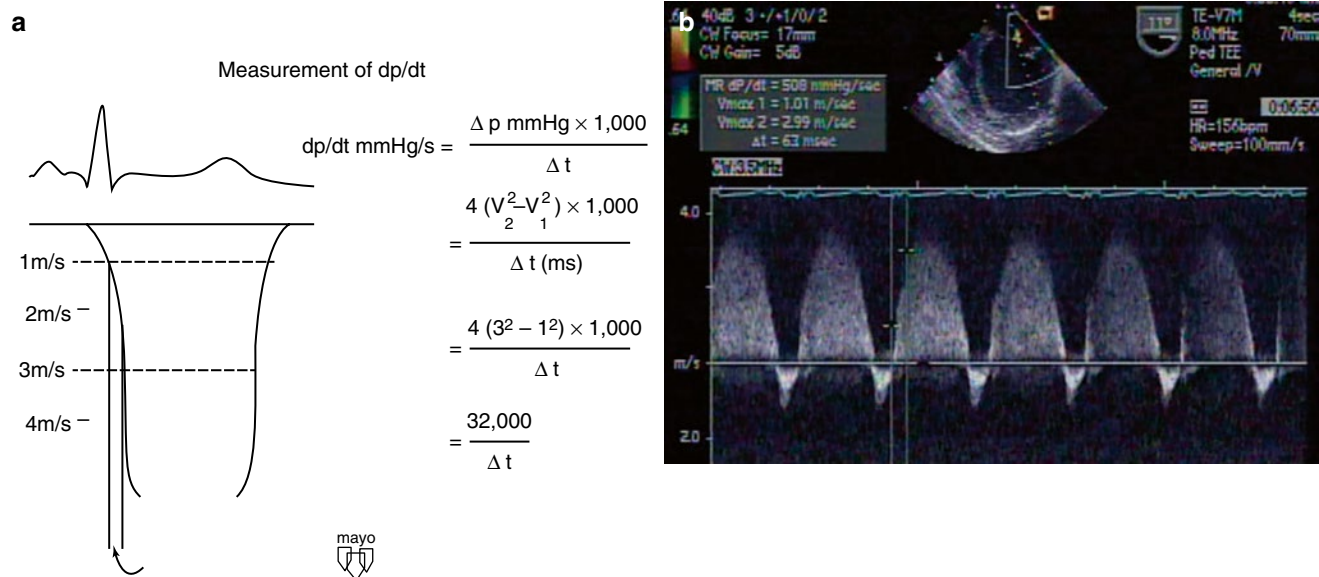
Fig. 5.4 Left ventricular dP/dt. (**a**) Measurement of dP/dt. (**b**) Calculation of left ventricular (LV) dP/dt from the mitral regurgitation (MR) jet. This still frame demonstrates the Doppler velocity curve of the MR jet obtained during TEE in a child with dilated cardiomyopathy and severe LV dysfunction. Utilizing the simplified Bernoulli equation, the LV dP/dt is the change in LV pressure measured from 1.0 to 3.0 m/s divided by the change in time between these two LV pressure points: LV dP/dt=(36 mmHg−4 mmHg)/63 ms=508 mmHg/s (normal >1,200 mmHg/s). Figure 5.4a used with permission from Mayo Clinic

correlates more accurately with invasive cardiac catheterization measurements. To ascertain peak LV dP/dt noninvasively, the MR signal is digitized to obtain the first derivative of the pressure gradient curve from which peak positive LV dP/dt can be calculated. While reflective of myocardial contractility, peak positive LV dP/dt is significantly affected by changes in preload and afterload [43, 82]. Peak negative LV dP/dt and the time constant of relaxation (Tau) can also be calculated from the MR signal, serving as indices of diastolic function.
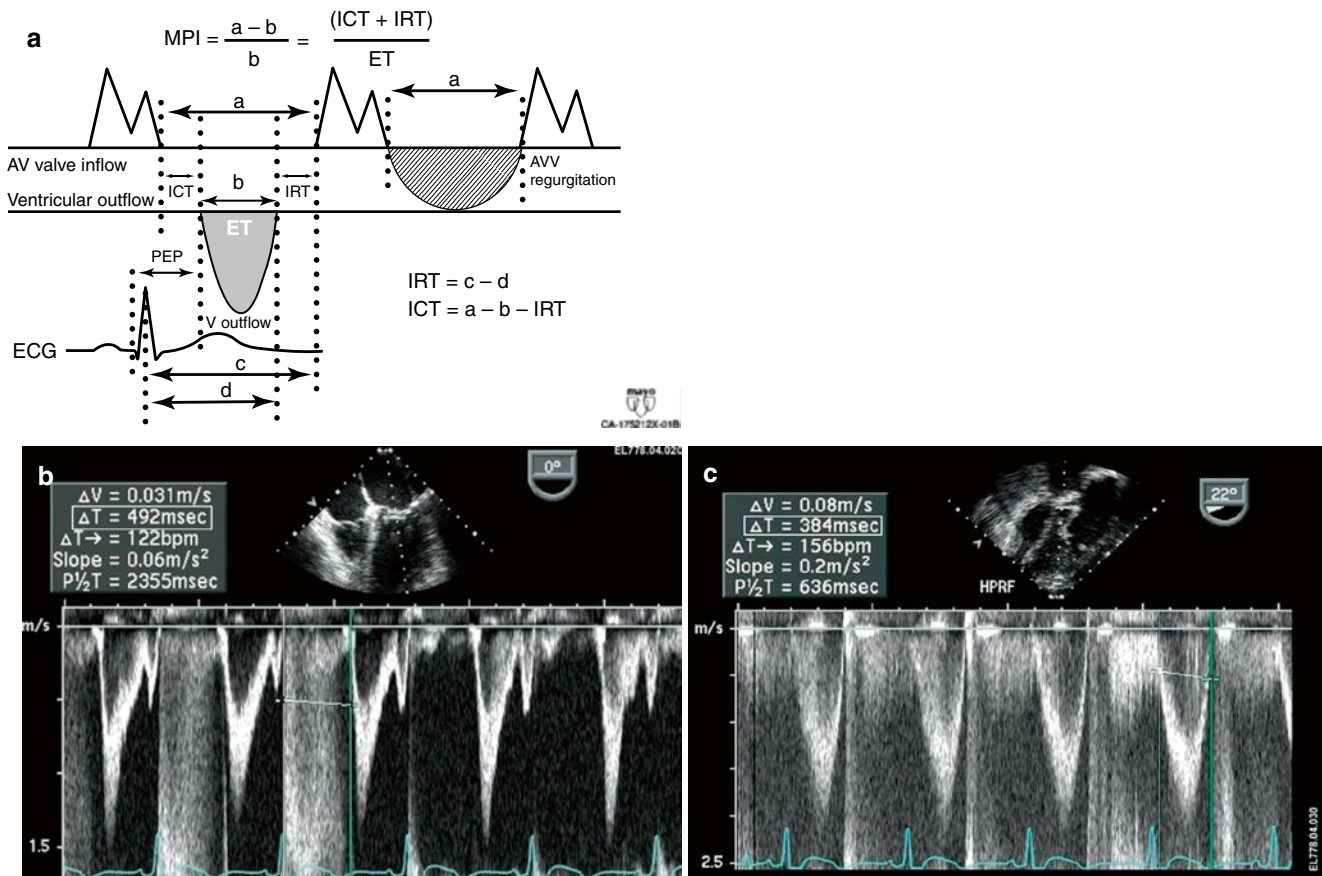
Myocardial Performance Index

The myocardial performance index (MPI), also referred to as Tei index, is a Doppler-derived quantitative measure of global ventricular function that incorporates both systolic and diastolic time intervals [83–87]. The MPI is defined as the sum of isovolumic contraction time (ICT) and isovolumic relaxation time (IRT) divided by ejection time (ET) (Fig. 5.5):

$$MPI = (ICT + IRT) / ET$$

The components of this index are measured from routine pulsed wave Doppler signals at the atrioventricular valve and ventricular outflow tract of either the LV or RV (as an alternative, the comparable signals from tissue Doppler imaging, as described below, can be used). To derive the sum of ICT and IRT, the Doppler derived ejection time for either ventricle is subtracted from the Doppler interval between cessation and onset of the respective atrioventricular valve inflow signal (from the end of the Doppler A wave to the beginning of the Doppler E wave of the next cardiac cycle). Increasing values of the MPI correlate with increasing degrees of global ventricular functional impairment.

Both adult and pediatric studies have established normal values for the MPI [84, 86, 88]. In adults, normal LV and RV MPI values are 0.39 ± 0.05 and 0.28 ± 0.04, respectively. In children, similar values for the LV and RV are reported to be 0.35 ± 0.03 and 0.32 ± 0.03, respectively. The MPI has been shown to be a sensitive predictor of outcome in adult and pediatric patients with acquired and CHD [85, 86, 89–94]. One of the advantages of the MPI is the ease in which it can be obtained, both by TTE as well as TEE. Because the MPI incorporates measures of both systolic and diastolic performance, this index may be a more sensitive early measure of ventricular dysfunction in the absence of other overt changes in isolated systolic or diastolic echocardiographic indices. In addition, because the MPI is a Doppler-derived index, it has been reported to be easily applied to the assessment of both LV and RV function as well as complex ventricular geometries in patients with CHD [89, 90, 92, 93]. The MPI, however, does have major limitations. It is significantly affected by changes in loading conditions, particularly preload, and has a paradoxical change with high filling pressures or severe semilunar valve regurgitation ("pseudo-normalization"). In addition, the combined nature of this index fails to readily discriminate between abnormalities of systolic or diastolic performance.

Fig. 5.5 Myocardial performance index (*MPI*) for assessment of left ventricular global function. *AV* atrioventricular, *AVV* atrioventricular valve, *ECG* electrocardiogram, *PEP* pre ejection period, *V* ventricular. (**a**) MPI represents the ratio of isovolumic contraction time (*ICT*) and isovolumic relaxation time (*IRT*) to ventricular ejection time (*ET*):

$$MPI = (ICT + IRT) / ET$$

(**b**) Mid esophageal four chamber view. The duration of ICT+IRT is measured from the cessation of mitral valve inflow to the onset of

atrioventricular valve inflow of the next cardiac cycle (interval a). (**c**) Deep transgastric view with pulsed wave Doppler within the left ventricular outflow tract. Ventricular ejection time is measured from the onset to cessation of LV ejection (interval b)

$$LV\ MPI = (492 - 384) / 384 = 0.28$$

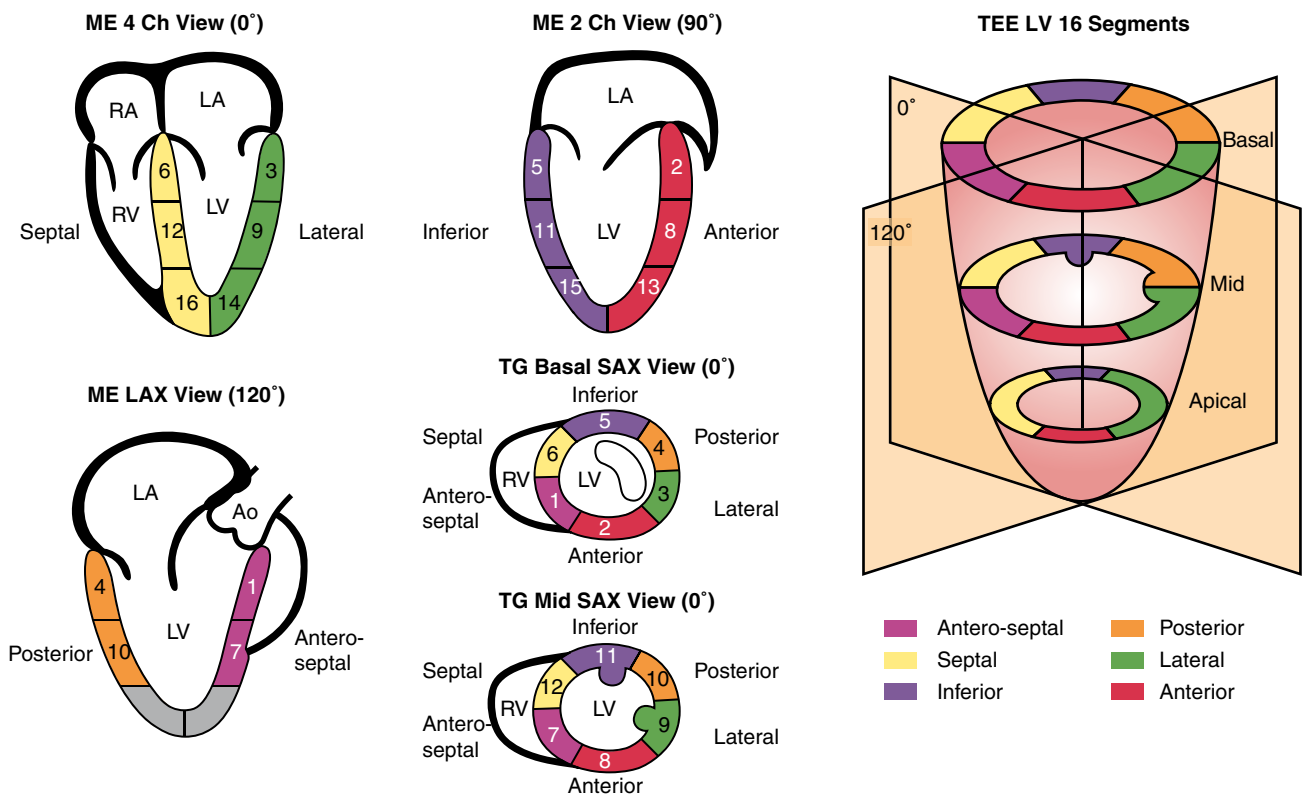(Figure a from Eidem et al. [88], with permission)

Echocardiographic Assessment of Regional Left Ventricular Systolic Function

Two-Dimensional Imaging

Regional ventricular function can be assessed by examining wall motion and systolic wall thickening. TEE, particularly in the intraoperative setting, is ideally suited for this purpose. Changes in ventricular wall motion typically occur during periods of decreased coronary perfusion, as can be the case during surgical interventions. These wall motion alterations are characterized by reduced systolic thickening and decreased inward endocardial excursion.

In order to facilitate regional wall function assessment several schemes have been proposed that include specific nomenclature, a variable number of LV segmental divisions, and different methods of wall motion analysis. Two models of LV segmental division have been favored as follows: (1) the 16-segment LV model and (2) the 17-segment LV model. The former, established in 1989 [16], represents an effort by the American Society of Echocardiography Committee on Standards and forms the basis for the recommendations in the original guidelines for performing a comprehensive intraoperative multiplane TEE examination established by the American Society of Echocardiography and the Society of Cardiovascular Anesthesiologists [95]. The latter, proposed by the American Heart Association in 2002, aimed to standardize myocardial segmentation and nomenclature for all types of cardiac imaging modalities [96]. These two models as applicable to TEE imaging are illustrated in Figs. 5.6 and 5.7.

ME 4 Ch View (0˚)

ME 2 Ch View (90˚)

TEE LV 16 Segments

ME LAX View (120˚)

TG Basal SAX View (0˚)

TG Mid SAX View (0˚)

Antero-septal · Posterior · Septal · Lateral · Inferior · Anterior

Fig. 5.6 SCA/ASE 16-segment model of the left ventricle

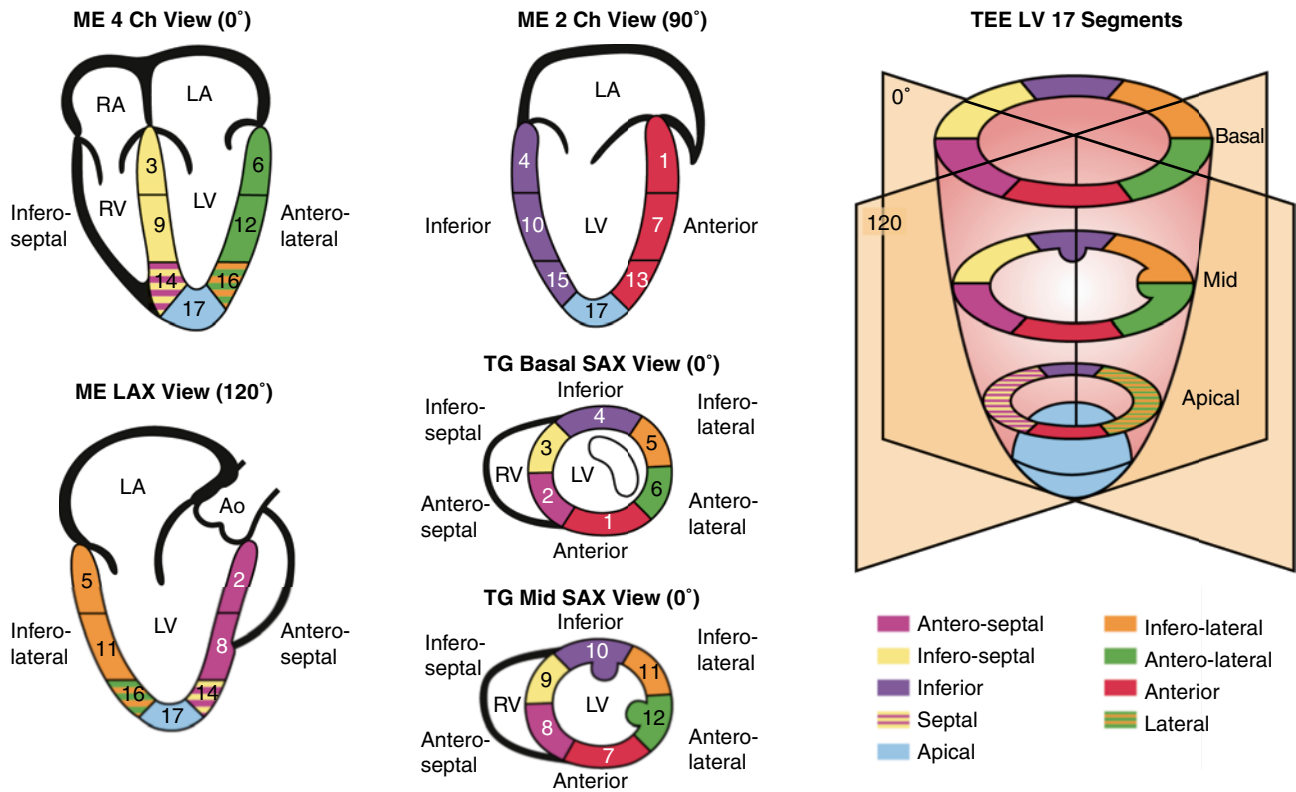| Basal segments	Mid segments	Apical segments
1. Basal antero-septal	7. Mid antero-septal	13. Apical anterior
2. Basal anterior	8. Mid anterior	14. Apical lateral
3. Basal lateral	9. Mid lateral	15. Apical inferior
4. Basal posterior	10. Mid posterior	16. Apical septal
5. Basal inferior	11. Mid inferior	
6. Basal septal	12. Mid septal	

Modified from Vegas [97], with permission from Springer

The 16-segment model divides the LV into three levels from base to apex: basal, mid, and apical. The basal and mid levels are each divided circumferentially into six segments, and the apical level into four. The 17-segment model added the apical cap or myocardial apex at the extreme tip of the LV beyond the chamber cavity. It was also suggested that the term 'inferior' might be more suitable than 'posterior' in reference to the ventricular walls. In the most recent recommendations for chamber quantification it is pointed out that the 16-segment model is more suitable for assessing wall motion abnormalities (as the apical segment does not move), while the 17-segment model is more appropriate for myocardial perfusion evaluation and comparison among various imaging modalities [97].

The TG Mid SAX view at the level of the papillary muscles is the suggested starting point to facilitate the qualitative evaluation of regional ventricular systolic function. Although there is significant variability in the myocardial blood supply by the coronary arteries, this cross-section allows for a prompt assessment of segmental wall function since all coronary artery territories are represented in this view (Fig. 5.8). Additional TEE cross-sections are needed to evaluate all myocardial segments as allowed by multiplanar imaging, including the ME 4 Ch, ME 2 Ch, and ME LAX views (Fig. 5.8). The visual assessment of wall motion should be graded as normal/hyperkinetic, hypokinetic (reduced systolic thickening), akinetic (absent systolic thickening), dyskinetic (paradoxical systolic motion), or aneurysmal (diastolic deformation).

The feasibility of this segmental functional analysis and its utility has been reported in infants with CHD. In a prospective study of neonates undergoing an arterial switch operation for transposition of the great arteries, segmental wall motion was examined in the TG Mid SAX and ME 4 Ch views [98]. The presence of severe wall motion abnormalities that persisted at the completion of surgery and were present in multiple segments was found to correlate with myocardial ischemia in this cohort. This highlights the importance of regional functional analysis in patients undergoing interventions that involve the coronary arteries, aortic root or any other procedures that can potentially impact coronary perfusion.

Fig. 5.7 AHA 17-segment model of the left ventricle

Basal segments	Mid segments	Apical segments
1. Basal anterior	7. Mid anterior	13. Apical anterior
2. Basal antero-septal	8. Mid antero-septal	14. Apical septal
3. Basal infero-septal	9. Mid infero-septal	15. Apical inferior
4. Basal inferior	10. Mid inferior	16. Apical lateral
5. Basal infero-lateral	11. Mid infero-lateral	17. Apex
6. Basal antero-lateral	12. Mid antero-lateral	

Modified from Vegas [97], with permission from Springer

Obviously, the two segmental models discussed apply principally to the LV in an anatomically "normal" heart—one with situs solitus, normal segments, and atrioventricular and ventriculoarterial connections (Chap. 4). As such, there will be limited direct application of these models for a number of congenital heart defects. Nonetheless the principles embodied in this segmental wall motion analysis—in particular, the evaluation of segmental wall kinetic motion—can be more generally applied to all forms of CHD. It facilitates a semi-quantitative, analytic assessment of wall motion and function even in hearts with very abnormal ventricular shape and morphology.

Tissue Doppler Imaging and Strain Rate Imaging

The assessment of regional systolic LV function, as detailed above, has centered upon the evaluation of segmental endocardial excursion and LV wall thickening. These semi-quantitative methods often fail to discriminate between active and passive myocardial motion. Newer echocardiographic modalities, including tissue Doppler imaging and strain rate imaging, offer a potentially more quantitative and accurate approach to the assessment of regional myocardial contraction and relaxation.

Tissue Doppler imaging (TDI, also known as Doppler tissue imaging or DTI) has been an addition to the armamentarium of the echocardiographer in recent years. By incorporating a high pass filter, tissue Doppler allows the display and quantitation of the low velocity high amplitude Doppler shifts present within the myocardium as opposed to the higher velocity lower amplitude Doppler signals more commonly measured within the blood pool (Fig. 5.9). Tissue Doppler echocardiography is less load-dependent than corresponding Doppler velocities from the blood pool and has systolic and diastolic components. These systolic velocities are heterogenous depending on ventricular wall and position.

Measurement of myocardial wall velocities by TDI has been shown to be a promising modality for assessment of longitudinal systolic performance [49, 51, 100]. Recent

ME 4 Ch View (0˚)   ME 2 Ch View (90˚)

ME LAX View (120˚)   TG Mid SAX View (0˚)

■ LAD   ■ Circumflex   ■ RCA
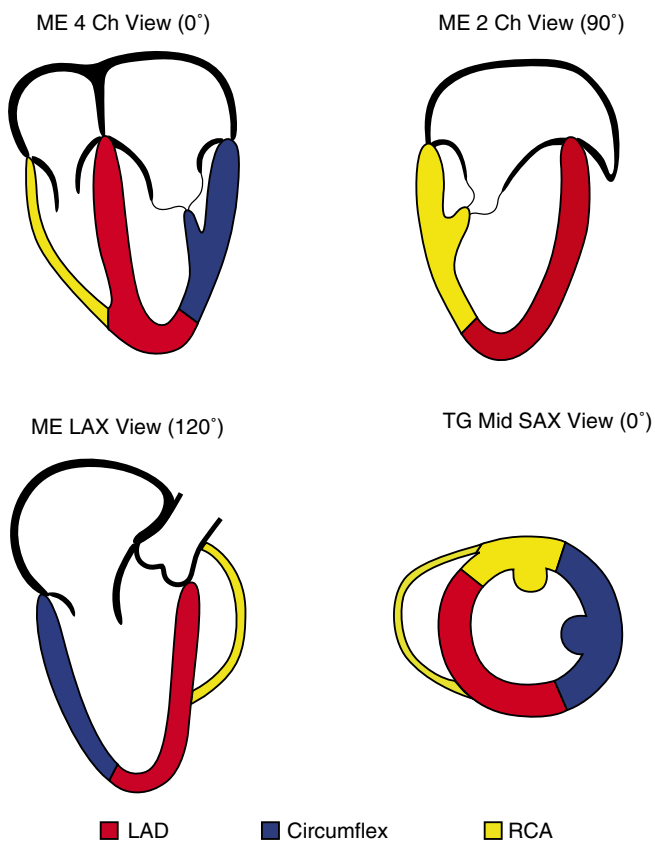
Fig. 5.8 Myocardial regions perfused by the major coronary arteries. The figure displays the typical myocardial territories perfused by the major coronary arteries

Left coronary circulation	Right coronary circulation
Left anterior descending (LAD) artery: (anterior, antero/infero septal walls)	Right coronary artery (RCA): (inferior wall, RV, SA and AV nodes)
Septal perforators	Posterior interventricular
Diagonal branches	Posterior Lateral
Posterior interventricular	Acute marginal
Circumflex (Cx) artery: (posterior, lateral walls)	Papillary muscles blood supply:
Obtuse marginal branches	AL by two arteries (obtuse + diagonal)
Posterior interventricular	PM by one artery (RCA or obtuse)

Dominance depends on which vessel (RCA or Cx) supplies the posterior interventricular branch. The majority of hearts (85 %) are right dominant. *AL* anterolateral, *AV* atrioventricular, *RV* right ventricle, *SA* sinotrial, *PM* posteromedial
Modified from Vegas [97], with permission from Springer

studies have demonstrated significant changes in mitral annular systolic TDI velocities in adult patients with LV dysfunction and elevated filling pressures [101, 102]. These indices have also been used to identify subclinical systolic ventricular dysfunction in pediatric patients [103]. Data in children following cardiac transplantation have also been found to correlate with hemodynamic parameters [104].

Tissue Doppler velocities, however, cannot differentiate between active contraction and passive motion, representing

a major limitation when assessing regional myocardial function. Regional strain rate corresponds to the rate of regional myocardial deformation and can be calculated from the spatial gradient in myocardial velocity between two neighbouring points within the myocardium. Regional strain represents the amount of deformation (expressed as a percentage) or the fractional change in length caused by an applied force and is calculated by integrating the strain rate curve over time during the cardiac cycle. Strain measures the total amount of deformation in either the radial or longitudinal direction while strain rate calculates the velocity of shortening (Fig. 5.10). These two measurements reflect different aspects of myocardial function and therefore provide complementary information. In contrast to tissue Doppler velocities, these indices of myocardial deformation are not influenced by global heart motion or tethering of adjacent segments and therefore represent better indices of true regional myocardial function.

Studies have demonstrated regional differences in strain rate in adult patients after myocardial infarction [50, 105]. Measurements of radial and longitudinal strain rate have also been reported in normal children [106]. In addition, quantification of regional RV and LV function by strain rate and strain indexes after surgical repair of tetralogy of Fallot in children demonstrated that RV deformation abnormalities are associated with electrical depolarization abnormalities or chronic pulmonary regurgitation [107–110]. Further studies are needed to identify potential applications of strain rate imaging and related newer modalities (speckle-tracking and vector velocity imaging) in the evaluation of ventricular mechanics and regional assessment of myocardial function of both right and left ventricles in children [111]. It is hoped that future investigations can address the suitability of these approaches in the perioperative setting.

## Echocardiographic Assessment of Diastolic Ventricular Function

2D and particularly Doppler echocardiography, have historically been essential noninvasive tools in the quantitative assessment of LV diastolic function. Abnormalities of ventricular compliance and relaxation can be demonstrated by characteristic changes in mitral inflow and pulmonary venous Doppler patterns [112]. Newer methodologies including tissue Doppler echocardiography and flow propagation velocities enhance the ability of echocardiography to define and quantitate these adverse changes in diastolic performance. Because diastolic dysfunction often precedes systolic dysfunction, careful assessment of diastolic function is mandatory in the noninvasive characterization and serial evaluation of patients with CHD.

Noninvasive evaluation of diastolic function in normal infants and children is influenced by a variety of factors
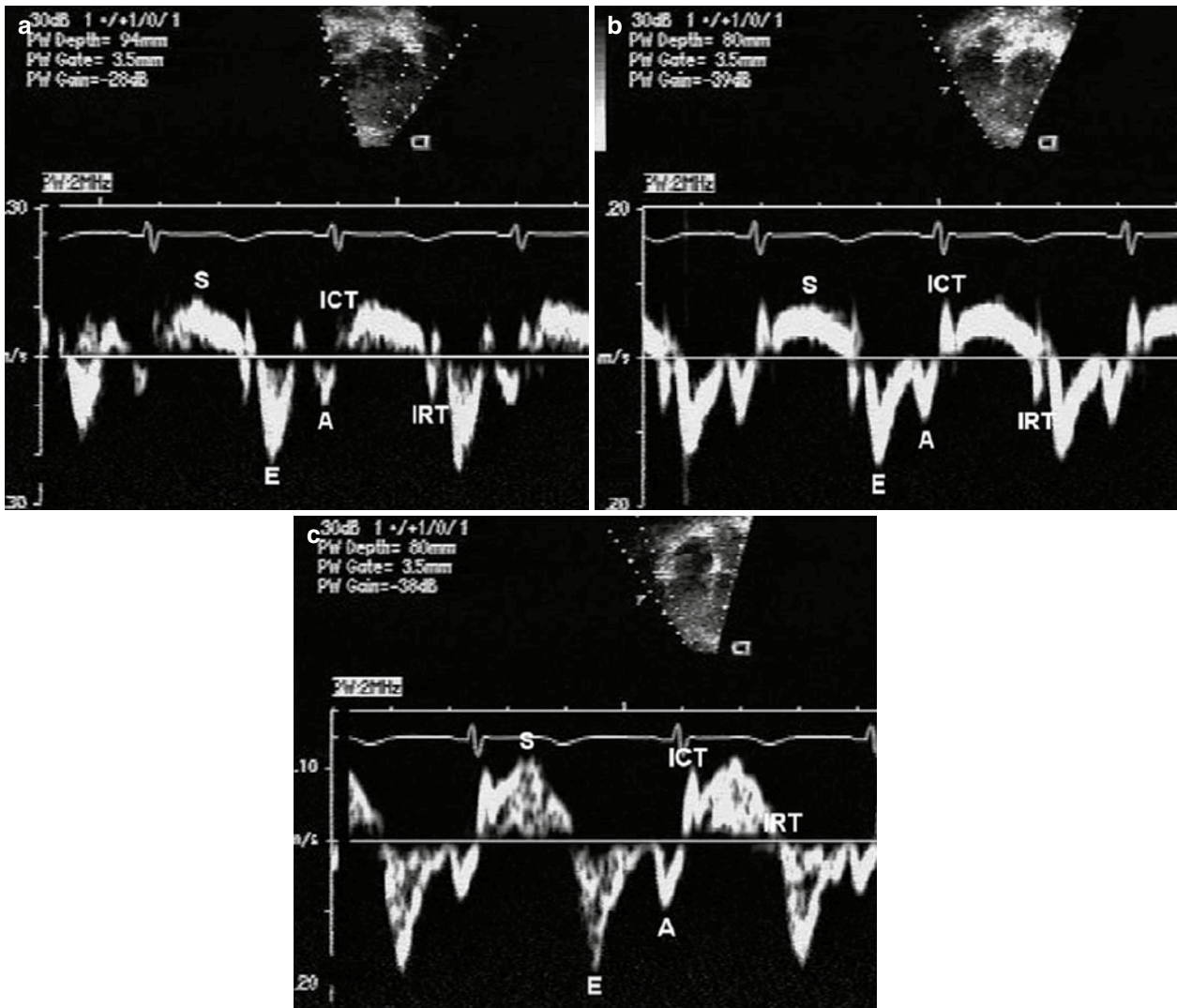
Fig. 5.9 Tissue Doppler imaging. Normal mitral annular (panel a), septal (panel b), and tricuspid annular (panel c) pulsed wave longitudinal Doppler tissue velocities. Note the characteristic normal pattern of a larger early diastolic velocity (E-wave) compared to late diastolic velocity (A-wave). The S-wave is the systolic wave. ICT, isovolumic contraction time; IRT, isovolumic relaxation time (From Eidem et al. [99], with permission)
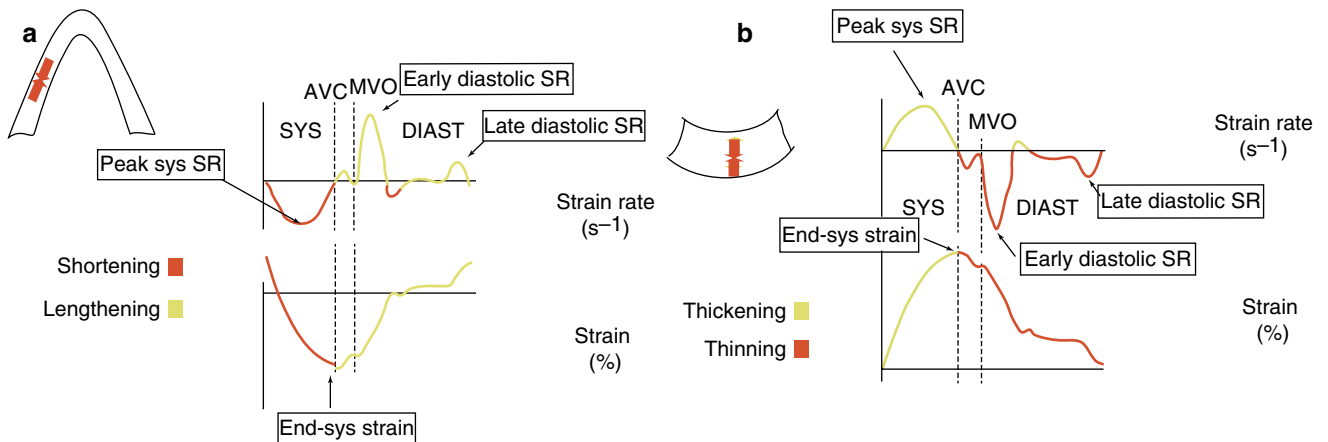
Fig. 5.10 Strain and strain rate imaging. Schematic representation of longitudinal (**a**) and radial (**b**) strain and strain rate imaging. In the longitudinal direction, strain represents myocardial shortening (systole) and lengthening (diastole) while strain rate represents the rate at which shortening or lengthening occurs. Similarly, radial strain represents myocardial thickening (systole) and thinning (diastole) while strain rate represents the rate at which thickening or thinning occurs. *AVC* aortic valve closure, *diast* diastole, *MVO* mitral valve opening, *SR* strain rate, *sys* systole/systolic (Figures used with permission from Luc Mertens, MD)

including age, heart rate, and the respiratory cycle. Reference values detailing both mitral and pulmonary venous Doppler velocities in a large cohort of normal children have been established using transthoracic imaging [113]. Similar to many echocardiographic parameters, these Doppler velocities are also significantly impacted by loading conditions making determination of diastolic dysfunction by using these parameters alone very challenging in patients with CHD.

Although the evaluation of diastolic function using TEE has been reported in adult patients in the perioperative setting, there are no formal studies addressing this application in the pediatric age group. The discussion that follows reviews general concepts of diastolic evaluation in children with the use of echocardiography and potential applications using the transesophageal modality.
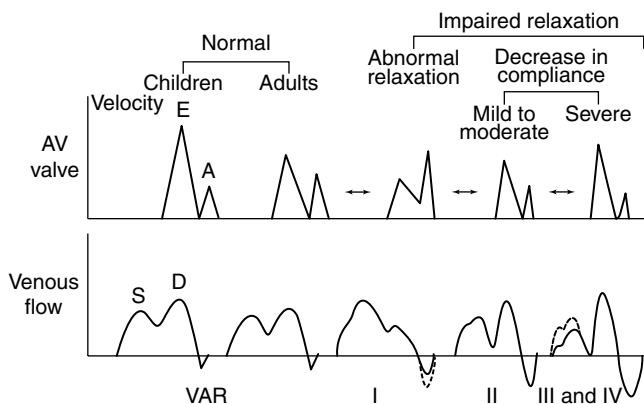
Mitral Inflow Doppler

Mitral inflow Doppler is readily obtained from the ME 4 Ch view and represents the diastolic pressure gradient between the left atrium (LA) and LV (Fig. 5.11). The early diastolic filling wave, or E-wave, is the dominant diastolic wave in children and young adults and represents the peak LA to LV pressure gradient at the onset of diastole. The deceleration time of the mitral E-wave reflects the time period needed for equalization of LA and LV pressures. The late diastolic filling wave, or A-wave, represents the peak pressure gradient between the LA and LV in late diastole at the onset of atrial contraction. Normal mitral inflow Doppler is characterized by a dominant E-wave, a smaller A-wave, and a ratio of E- and A-waves (E:A ratio) between 1.0 and 3.0. Normal duration of mitral deceleration time as well as isovolumic relaxation time vary with age and have been reported in both

pediatric and adult populations [113, 115–118]. Mitral inflow Doppler velocities are not only impacted by changes in LV diastolic function but also by a variety of additional hemodynamic factors including age, altered loading conditions, heart rate, and changes in atrial and ventricular compliance. Interpretation of characteristic patterns of mitral inflow must be carefully evaluated with particular attention paid to the potential impact of each of these hemodynamic factors on the Doppler velocities.

The earliest stage of LV diastolic dysfunction demonstrated by mitral inflow Doppler is abnormal relaxation (Fig. 5.11). This Doppler pattern is characteristic of normal aging in adults and represents a mild decrease in the rate of LV relaxation with continued normal LA pressure. It is characterized by a reduced E-wave velocity, increased A-wave velocity, decreased E:A ratio <1.0, and a prolonged mitral deceleration time and isovolumic relaxation time (IVRT).

As diastolic dysfunction progresses, further changes in ventricular relaxation and compliance occur leading to an increase in LA pressure. Increased LA pressure normalizes the initial transmitral gradient between the LA and LV producing a "pseudo-normalized" mitral inflow Doppler pattern with increased E-wave velocity and E:A ratio, and normalized mitral deceleration and isovolumic relaxation time intervals (Fig. 5.11). This pseudo-normal Doppler pattern may be difficult to distinguish from normal mitral inflow Doppler; however, maneuvers that decrease ventricular preload, like the Valsalva maneuver, will uncover the underlying abnormalities of mitral inflow Doppler. In addition, evaluation of pulmonary venous inflow Doppler can help unmask this advanced degree of LV diastolic dysfunction (see below).

Further deterioration of LV diastolic function results in restrictive ventricular filling with an additional increase in LA pressure and a concomitant decrease in ventricular compliance. The Doppler pattern of restrictive LV filling is characterized by additional increases in E-wave velocity, reduction in A-wave velocity, an increased E:A ratio >3.0, and significant shortening of both mitral deceleration time and IVRT (Fig. 5.11) [115]. This pattern is typically seen in patients with restrictive cardiomyopathy and may also be seen in other conditions associated with restrictive physiology (i.e., acute post-transplant setting).

Fig. 5.11 Doppler patterns in diastolic dysfunction. Graphic representation of spectrum of changes in mitral and pulmonary venous inflow patterns associated with diastolic dysfunction in children. *A* atrial filling wave, *AV* atrioventricular, *D* pulmonary vein diastolic flow wave, *E* early filling wave, *S* pulmonary vein systolic flow wave, *VAR* vein atrial reversal wave (Modified from: Olivier et al. [114], with permission)
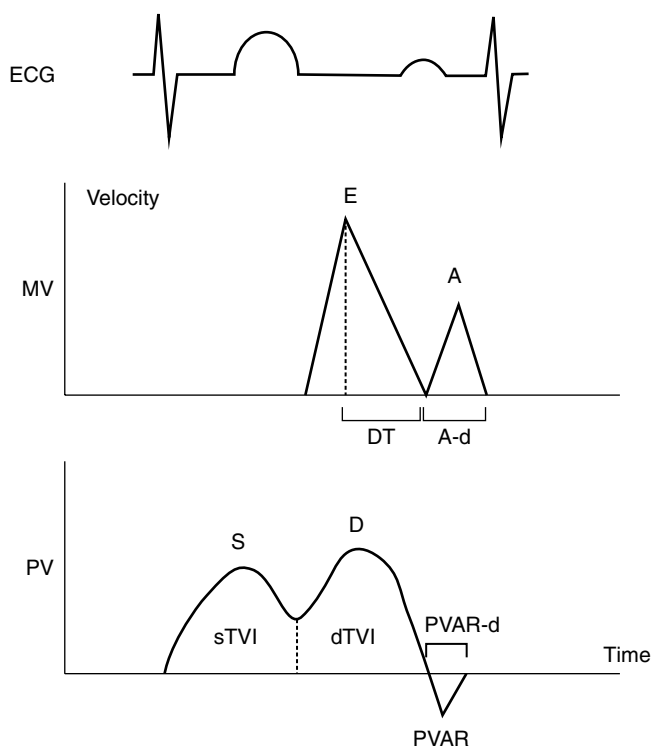
Pulmonary Venous Doppler

Pulmonary venous Doppler, combined with mitral inflow Doppler, provides a more comprehensive assessment of LA and LV filling pressures (Fig. 5.11) [119–121]. TEE is ideally suited to the acquisition and quantitation of pulmonary venous flows, particularly in patients with poor transthoracic windows [19, 20, 27, 122]. Pulmonary venous inflow consists of three distinct Doppler waves: a systolic wave (S-wave),

a diastolic wave (D-wave), and a reversal wave that occurs with atrial contraction (Ar-wave). In normal adolescents and adults, the characteristic pattern of pulmonary venous inflow consists of a dominant S-wave, a smaller D-wave, and a small Ar-wave of low velocity and brief duration. In neonates and younger children, a dominant D-wave is often present with a similar brief low velocity, or even absent, Ar-wave.

With worsening LV diastolic dysfunction, LA pressure increases leading to diminished systolic forward flow into the LA from the pulmonary veins with relatively increased diastolic forward flow resulting in a diastolic dominance of pulmonary venous inflow (Fig. 5.11). More importantly, both the velocity and duration of the pulmonary venous atrial reversal wave are increased. Pediatric and adult studies have demonstrated that an Ar-wave duration >30 ms longer than the corresponding mitral A-wave duration or a ratio of pulmonary venous Ar-wave to mitral A-wave duration >1.2 is predictive of elevated LV filling pressure (Fig. 5.12) [113, 120]. Pulmonary venous flow variables as measured by TEE have been correlated with estimations of mean LA pressure in adults undergoing cardiovascular surgery [19].

Fig. 5.12 Mitral valve and pulmonary venous Doppler tracings. Diagram depicting mitral valve (*MV*) and pulmonary vein (*PV*) Doppler flow tracings. *A* atrial filling wave, *A-d* duration of atrial filling wave, *D* pulmonary vein diastolic flow wave, *DT* mitral deceleration time, *dTVI* time velocity integral of pulmonary vein diastolic flow wave, *E* early filling wave, *ECG* electrocardiogram, *PVAR* pulmonary vein atrial reversal wave, *PVAR-d* duration of pulmonary vein atrial reversal flow, *S* pulmonary vein systolic flow wave, *sTVI* time velocity integral of pulmonary vein systolic flow wave (From O'Leary et al. [113], with permission)

Tissue Doppler Imaging

Tissue Doppler imaging is particularly well suited to the quantitative evaluation of LV diastolic function and can be easily obtained by either a transthoracic or transesophageal approach. Both early (Ea) and late (Aa) annular diastolic velocities can be readily obtained by tissue Doppler echocardiography (Fig. 5.9). Similar to systolic tissue Doppler velocities, differences in diastolic velocities exist between (1) the subendocardium and subepicardium, (2) from cardiac base to apex, and (3) between various myocardial wall segments. Previous studies have reported an excellent correlation between the early annular diastolic mitral velocity and simultaneous invasive measures of diastolic function at cardiac catheterization [123]. Early annular diastolic velocities also appear to be less sensitive to changes in ventricular preload compared to the corresponding early transmitral Doppler inflow velocity [101, 123, 124]. These diastolic tissue Doppler velocities, however, are impacted by significant alterations in preload. The influence of afterload on tissue Doppler velocities is less controversial with many studies documenting significant changes in systolic and diastolic annular velocities with changes in ventricular afterload [125–127]. Therefore, the clinical use of tissue Doppler velocities in patients with valvar stenoses or other etiologies of altered ventricular afterload need to be interpreted carefully in light of this limitation.

Tissue Doppler velocities have been shown to be clinically helpful in the discrimination between normal and abnormal transmitral Doppler filling patterns [101, 128–130]. In addition to changes incurred by loading conditions, alterations in LA pressure as well as LV end-diastolic pressure also affect the early transmitral diastolic velocity. However, the corresponding tissue Doppler velocity is characteristically decreased in patients with pseudo-normal filling allowing differentiation of this abnormal filling pattern from one of normal transmitral Doppler inflow. Clinical reports have suggested a ratio of the early transmitral inflow Doppler signal to the lateral mitral annular early diastolic velocity (mitral E/Ea) as a noninvasive measure of LV filling pressure. Nagueh and colleagues demonstrated a significant correlation of mitral E/Ea with invasively measured mean pulmonary capillary wedge pressure [101], and subsequent studies have further validated this ratio and reported its applicability in a variety of hemodynamic settings mostly in adult populations. Additional novel indices of LV diastolic function utilizing tissue Doppler echocardiography have been reported that may further expand the role of this modality in the clinical evaluation of LV filling pressures [130, 131].

Tissue Doppler has also been shown to be of considerable clinical value in the differentiation of constrictive from restrictive LV filling [132–135]. Evaluation of patients with constrictive pericarditis and restrictive cardiomyopathy with 2D echocardiography and even invasive cardiac catheteriza-

tion may fail to confidently distinguish these two disease states. Because the myocardium in patients with constrictive pericarditis is most commonly normal, the corresponding tissue Doppler velocities are also normal. However, patients with restrictive cardiomyopathy have been shown to have significantly decreased early diastolic as well as systolic tissue Doppler velocities. Therefore evaluation of tissue Doppler velocities allows separation of these two distinct clinical entities.

## Tissue Doppler Studies in Normal Children

A number of TTE studies have been performed in children to establish normal reference values of tissue Doppler velocities in this cohort [99, 136–141]. Similar to previously published adult reports, pediatric tissue Doppler velocities vary with age, heart rate, wall location, and myocardial layer. In addition, pulsed wave tissue Doppler velocities are also highly correlated with parameters of cardiac growth, most notably LVEDD and LV mass with the most significant changes in these velocities occurring during the first year of life (Fig. 5.13) [99]. In a published large series of infants and children, tissue Doppler velocities did not correlate significantly with other more commonly utilized measures of systolic and diastolic ventricular performance including LV fractional shortening, LV and RV MPI, and transmitral inflow Doppler [99]. This lack of correlation in part is likely due to pulsed wave tissue Doppler assessing longitudinal ventricular function while other more traditional 2D and Doppler methods assess radial and global measures of ventricular performance.

Similar to previously published adult normative data, normal values for the E/Ea ratio in children have also been
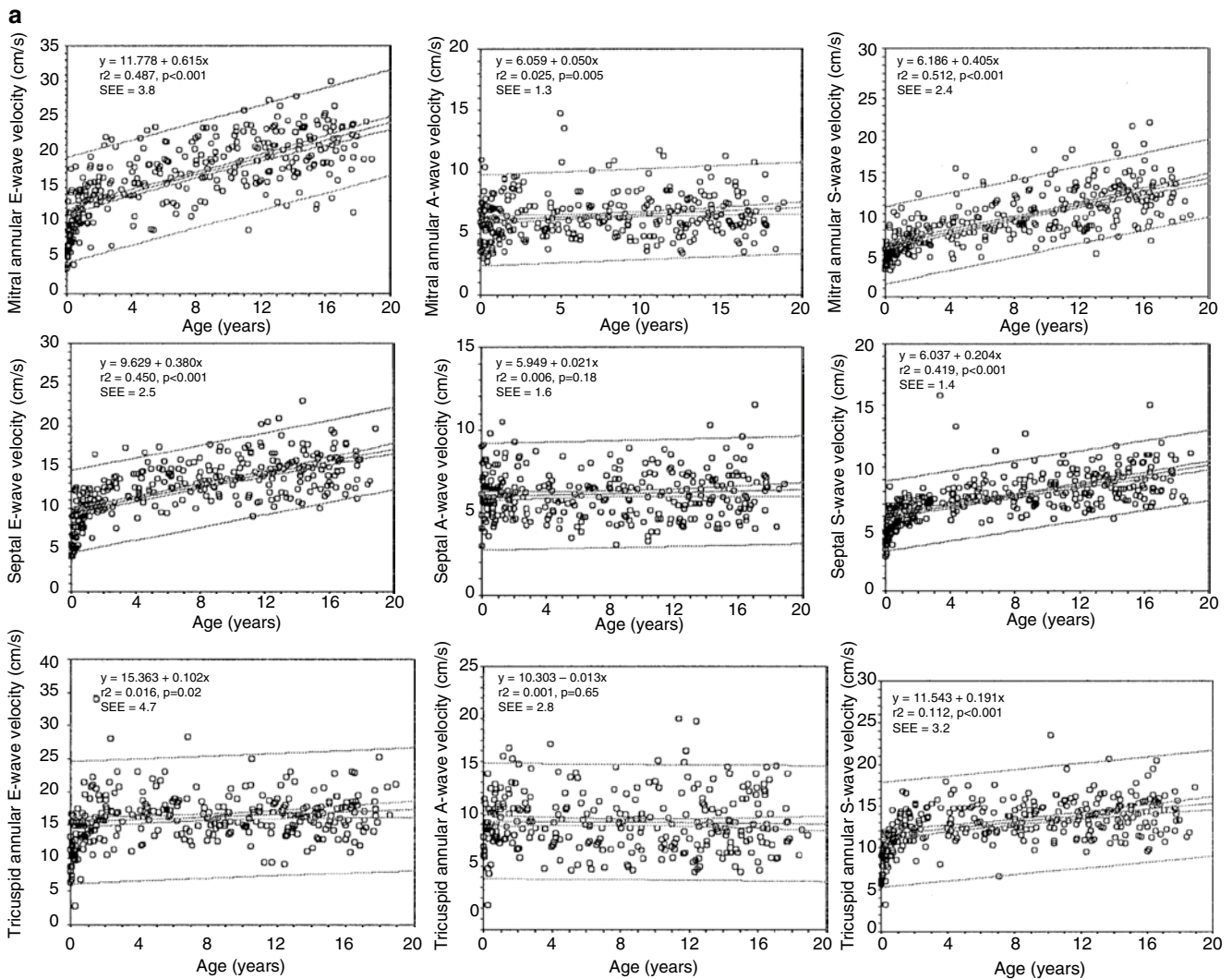
Fig. 5.13 Tissue Doppler velocities in children. Influence of age (**a**) and left ventricular end-diastolic dimension (**b**) on longitudinal systolic (S) and diastolic (E and A) pulsed wave tissue Doppler velocities in children (From: Eidem et al. [99], with permission)

b
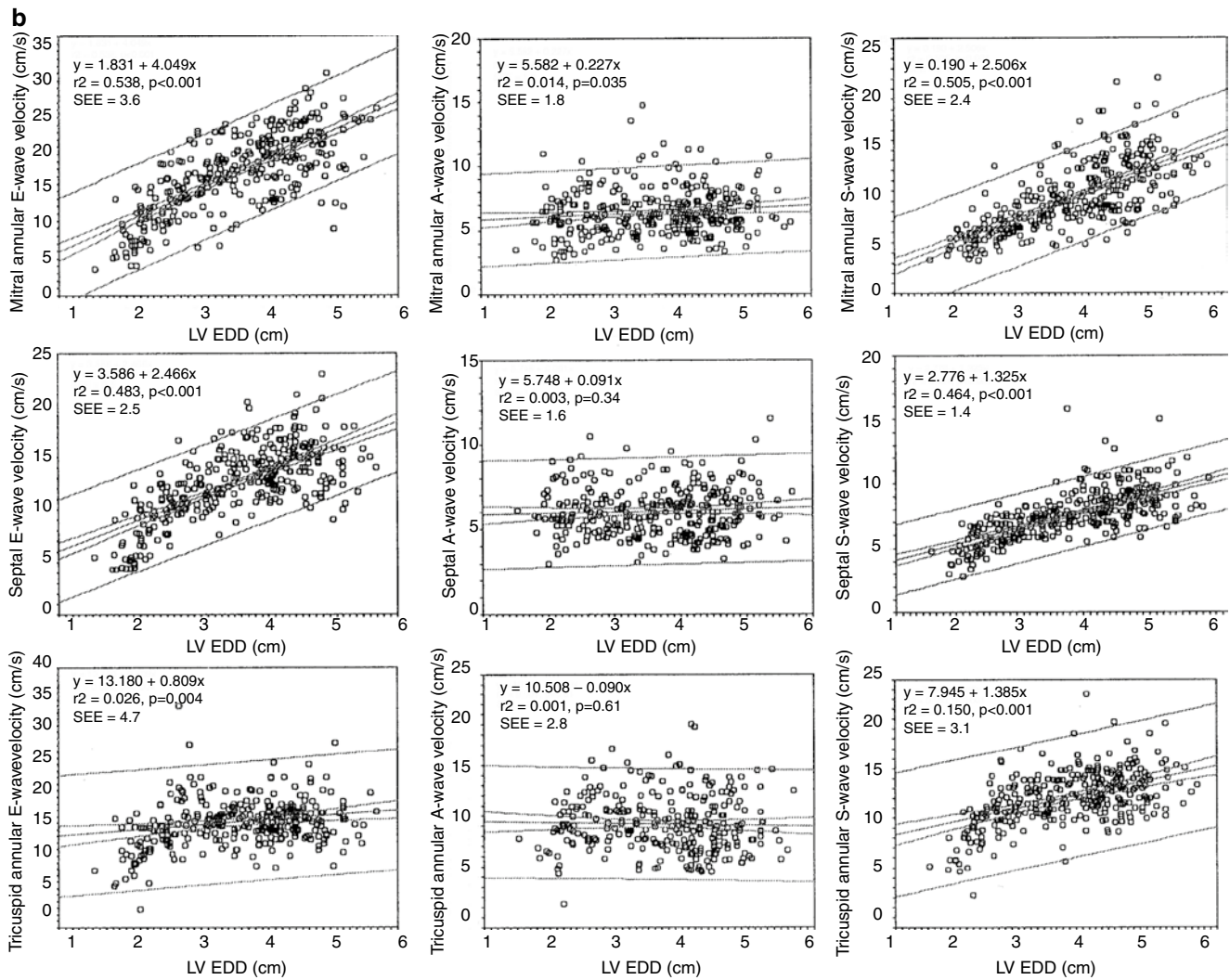
Fig. 5.13 (continued)

reported [99]. These values are also impacted by age, heart rate, ventricular wall location, LV dimension, and LV mass. Values for E/Ea are highest in neonates and decrease with advancing age primarily due to an increased Ea velocity over this time period. Data regarding simultaneous catheterization—echocardiographic measurements correlating the E/Ea ratio in children with invasive measures of LV filling pressure are limited to date. Two recent studies in children following cardiac transplantation demonstrate a poor correlation between these parameters. One study found E:E′ to be a poor predictor of simultaneously obtained, catheter-derived hemodynamic parameters in post-transplant children [142]. Another recent study reported that E/Ea does not correlate well with filling pressures observed after pediatric heart transplantation [104]. However, a septal E/Ea > 12 was associated with elevated pulmonary capillary

wedge pressure and high-grade cellular rejection. In addition, a lateral tricuspid E/Ea > 10 was associated with elevated mean right atrial pressure. In a small cohort of children, invasive cardiac catheterization measures of LV function were compared to simultaneously obtained color M-mode and Doppler parameters of LV performance [139]. The ratio of early diastolic mitral annular tissue Doppler velocity to flow propagation velocity (Ea/Vp) correlated closely with invasive LV end-diastolic pressure while the septal Ea velocity correlated with the time constant of relaxation (Tau). Additional studies utilizing tissue Doppler to establish normal atrioventricular electromechanical coupling intervals have also been reported [141]. The applications and clinical value of tissue Doppler echocardiography obtained by transesophageal imaging deserve further evaluation.
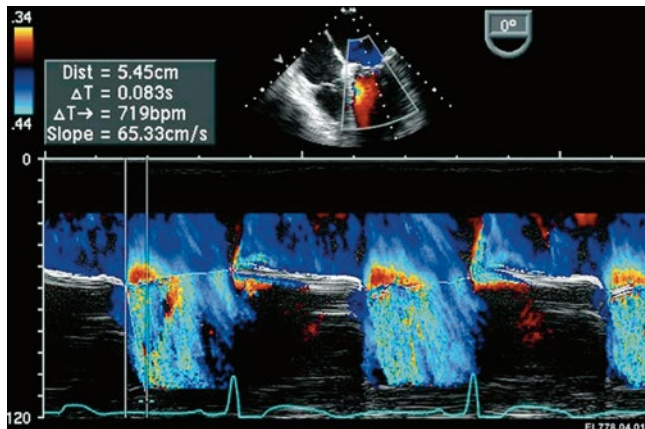
Fig. 5.14 Color M-mode Doppler flow propagation velocity. Measurement of flow propagation velocity (Vp) from color M-mode Doppler in the assessment of LV diastolic function. Vp is determined by the slope of the first clearly demarcated aliasing velocity (*white line*) during early left ventricular filling. In this 28 year old patient with aortic regurgitation, color M-mode during the intraoperative TEE examination demonstrated a normal Vp of 65 cm/s

Color M-Mode Flow Propagation Velocity

Flow propagation of early diastolic filling from the mitral annulus to the cardiac apex can be quantitated by color M-mode (Fig. 5.14). As opposed to mitral inflow Doppler, this propagation velocity has been shown to be significantly less affected by changes in heart rate, LA pressure, and loading conditions, and may therefore more accurately reflect changes in myocardial relaxation. Numerous studies have demonstrated a significant decrease in flow propagation velocity in patients with diastolic dysfunction of varying etiology [102, 143–145]. In addition, the ratio of the mitral annular Doppler tissue E-wave velocity to flow propagation velocity has also been shown to be a significant predictor of congestive heart failure and outcome in patients after myocardial infarction. This ratio of flow propagation and Doppler tissue imaging velocity may also be helpful in distinguishing a normal mitral inflow pattern from one of pseudo-normalized mitral inflow. In a small cohort of children undergoing simultaneous cardiac catheterization and TTE, Border and colleagues demonstrated a significant positive correlation between invasively measured LV end-diastolic pressure and the ratio of peak early transmitral Doppler flow velocity to flow propagation velocity (E/Vp) [146].

Echocardiographic Assessment of Right Ventricular Function

Echocardiographic assessment of RV function, either by transthoracic or transesophageal methods, has been limited due to the geometric shape of the RV. Doppler echocardiography has historically been useful in the noninvasive prediction of RV systolic and pulmonary artery pressures [147, 148].

However, quantification of RV systolic function by M-mode or 2D echocardiography has relied on the visual assessment of relative RV wall motion or semi-quantitative measurements of FAC in RV dimension or volume. Newer echocardiographic modalities that have shown promise in quantifying RV function include Doppler measures of RV performance (myocardial performance index, RV dP/dt, and Doppler tissue imaging) as well as acoustic quantification and 3D echocardiography.

Right Ventricular Myocardial Performance Index

As described previously, the MPI is a Doppler-derived measure of global ventricular function that can be applied to any ventricular geometry. Studies have validated the ability of the MPI to quantitatively assess RV function in adults and patients with CHD [88, 92]. In addition, the MPI has demonstrated prognostic power in discriminating outcome in patients with either RV or LV failure [89–91]. Care, however, must be exercised in using this index in patients with CHD with altered RV preload or afterload [55, 56, 149, 150]. The RV MPI has been shown to be relatively independent of changes in chronic loading conditions but the impact of acute changes in physiologic loading are significant and need further definition.

Right Ventricular dP/dt

Similar to the LV, the rate of pressure change over time can also be used as a measure of RV systolic function in patients with tricuspid regurgitation. RV dP/dt has been shown to correlate with invasive measures of RV performance [151–154]. RV dP/dt has also been demonstrated to be helpful in the serial assessment of RV function in children with hypoplastic left heart syndrome [153]. Similar to LV limitations with this parameter, RV dP/dt is impacted by changes in loading conditions.

Right Ventricular Tissue Doppler Imaging

Tissue Doppler imaging represents one of the most recent modalities applied to the quantitative evaluation of RV function. Tricuspid annular motion has been shown to correlate with RV function in previous studies [99, 137, 138, 140]. TDI has been reported to be a reproducible noninvasive method of assessing systolic and diastolic annular motion and RV function. While impacted by both afterload and preload, data in adults and children with TDI have demonstrated these velocities to be less influenced by altered preload than corresponding mitral or tricuspid inflow Doppler. Limited data is available regarding the applications of RV TDI in CHD [155].

Acoustic Quantification and Right Ventricular Function

Acoustic quantification utilizes automated border detection techniques to measure the absolute change and rate of change in RV volume. This modality has been shown to correlate with other invasive methods of RV functional assessment in adults with abnormalities of global RV function. Automated border methods have also shown good correlation with magnetic resonance imaging in assessing changes in RV volume and systolic function. Feasibility of acoustic quantification in the noninvasive transthoracic evaluation of RV function in normal children has also been reported [156, 157]. Ongoing investigation is needed to establish the potential of this technique for the identification and serial evaluation of RV dysfunction in children with the use of TEE.

Three-Dimensional Echocardiography and Right Ventricular Function

3D echocardiography has enabled the noninvasive evaluation of RV volume and function [158–160]. The ability of 3D echocardiography to evaluate RV geometry in multiple spatial planes allows for accurate assessment of changes in RV volume during the cardiac cycle. Application of live 3D TEE to the assessment of RV volume and systolic function in adults and children appears promising [161–164].

Echocardiographic Assessment of Single Ventricular Function in Patients with Complex Congenital Heart Disease

Quantitative measurement of ventricular function in patients with functional single ventricles can be challenging. In most cases, a visual estimate of systolic function from 2D images is used. Quantitative echocardiographic assessment is limited by complex ventricular geometry often with associated abnormalities of wall motion [165–167].

Similar to novel techniques used to assess RV function; Doppler echocardiography holds promise in the potential evaluation of global single ventricle function [114, 168–170]. However, only limited studies to date have addressed either dP/dt or the MPI in patients with functional single ventricles [93, 153, 171]. Data is lacking on the ability of these new Doppler indices to predict outcome in patients with complex single ventricle anatomy. Finally, 3D echocardiography also holds promise in the nongeometric assessment of ventricular volume and function but has yet to be comprehensively evaluated in patients with CHD with transesophageal imaging.

Summary

The assessment of ventricular performance in congenital pathology has been hindered by the fact that most cardiovascular anomalies are associated with abnormal ventricular geometry and altered loading conditions. Thus the application of classic parameters developed and widely utilized in the functional assessment of the structurally normal heart may not be suitable in the setting of CHD. The recently developed echocardiographic techniques discussed throughout this chapter have provided new insight into the functional abnormalities that may be present in this patient group. These modalities, initially investigated and applied during transthoracic imaging, should now allow for the functional assessment during TEE to evolve further from a qualitative to a more quantitative approach. The techniques described in this chapter, as well as promising techniques and technologies of the future such as 3D imaging, give hope towards being able to provide more detailed insights into the systolic and diastolic function in CHD patients with even the most complex cardiac anatomy and geometry.

Case Examples

Editor's Note: Several of the TEE images in this section (Videos 5.1b, 5.1d, 5.1e, 5.2b, 5.3d; Figs. 5.15a, b, 5.16a, 5.17) are displayed in a vertically inverted orientation with respect to equivalent views presented in Chap. 4 – Structural Evaluation and throughout the textbook. This represents a preference by some institutions to display TEE images in an orientation that mimics the equivalent transthoracic cross-sections.

Case 1

11 year old child referred for surgical closure of moderate-sized secundum atrial septal defect

Preoperative (Videos 5.1a, 5.1b) and postoperative TEE images (Videos 5.1c, 5.1d, 5.1e) from multiple views allow for qualitative assessment of ventricular size and function in this patient. The transgastric mid LV view as shown is Fig. 5.15 (Video 5.1e) provides for M-mode interrogation and determination of LV shortening fraction.

Case 2

22 year old patient with long QT syndrome referred for surgical excision of intracardiac right ventricular lead

Qualitative assessment of right and left ventricular systolic function by TEE in this case is displayed in Videos 5.2a and 5.2b. Representative M-mode images for determination of LV shortening fraction are shown in Figs. 5.16a and 5.16b; Doppler tracings obtained for calculation of LV MPI are illustrated in Figs. 5.16c and 5.16d.
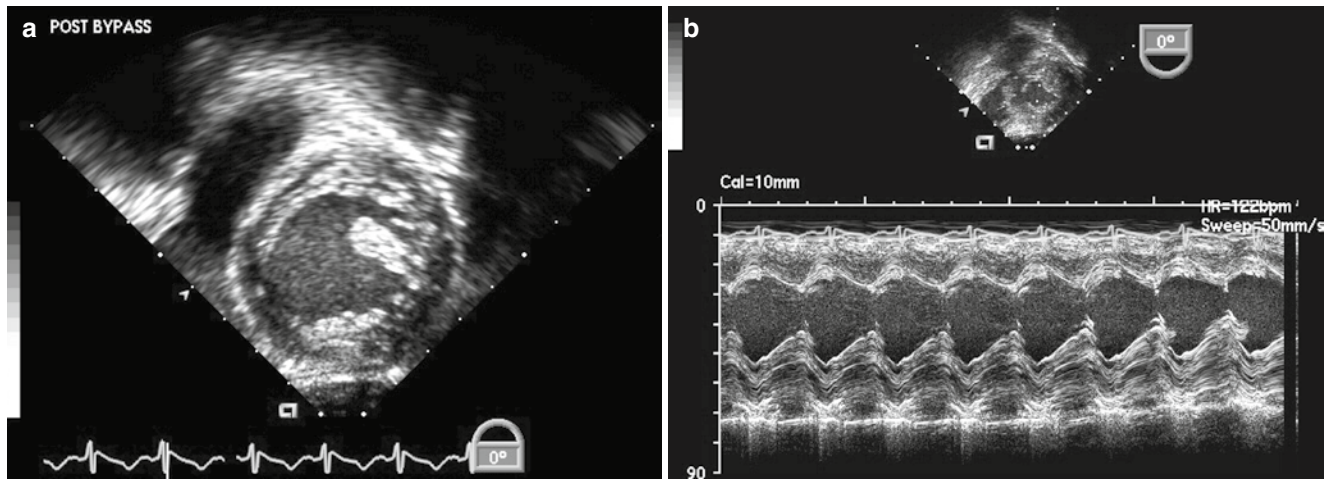
Fig. 5.15 (**a**) Still frame demonstrating the *elliptical shape* of the left ventricle in a transgastric view as shown in Video 5.1e. (**b**) Representative M-mode obtained during the TEE examination. The LV shortening fraction was 36 %. Note that the orientation of the M-mode beam with respect to the left ventricle during transesophageal/transgastric imaging may not correlate with that obtained during a transthoracic study
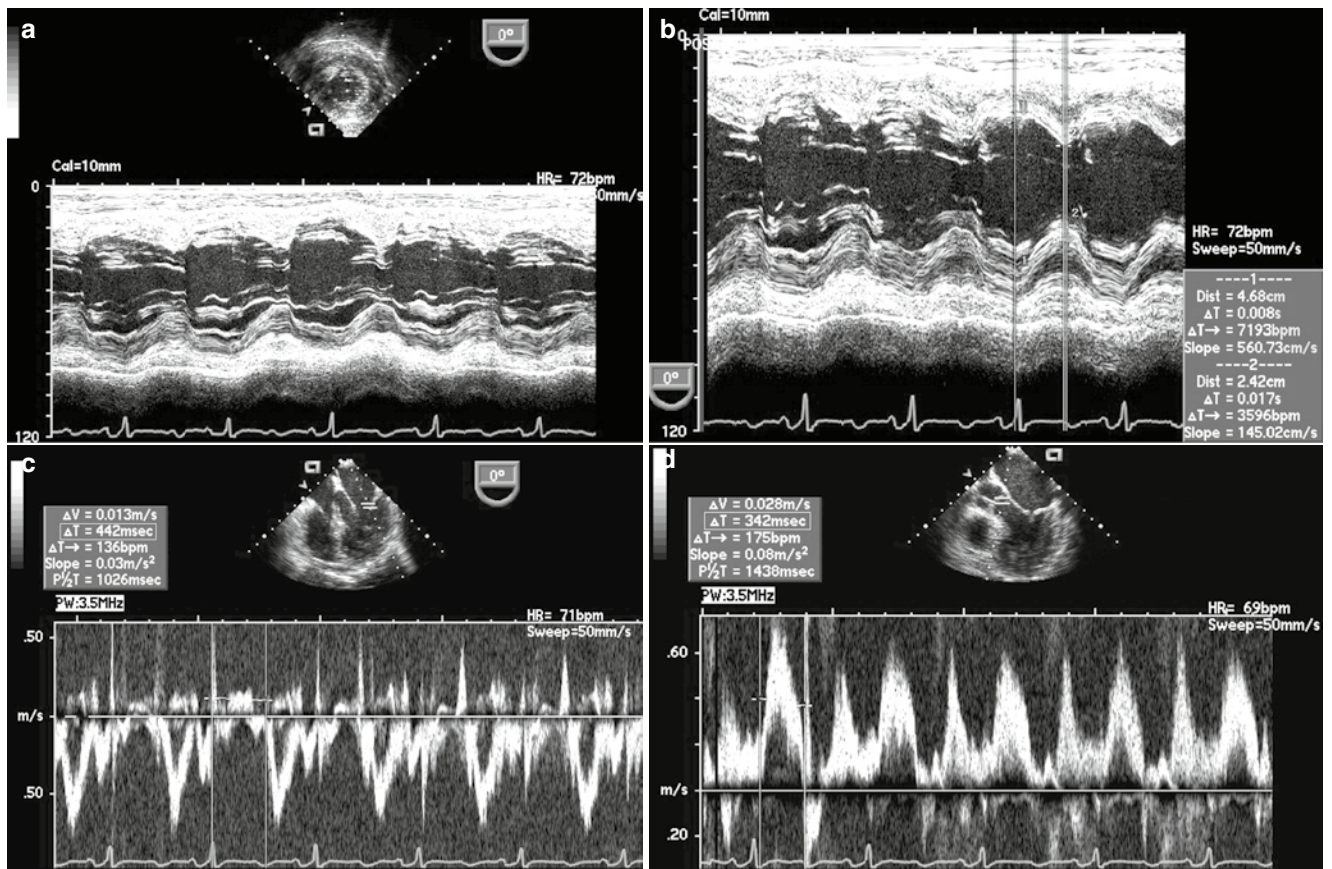
Fig. 5.16 (**a**, **b**) Representative M-mode images obtained during the TEE examination. The LV shortening fraction is = [(LVEDD) − (LVESD)]/(LVEDD) = [(47 mm) − (24 mm)]/(47 mm) = 49 %. (**c**, **d**) Measurement of the left ventricular myocardial performance index. (**c**) A pulsed wave Doppler signal is placed within the mitral valve inflow to obtain the mitral closure to opening interval (MV C-O, 442 ms). (**d**) A pulsed wave Doppler signal is placed within the left ventricular outflow tract to derive the ejection time (LVET, 342 ms). LV MPI = [(MV C-O) − (LVET)]/LVET = [(442 ms) − (342 ms)]/342 ms = 0.29
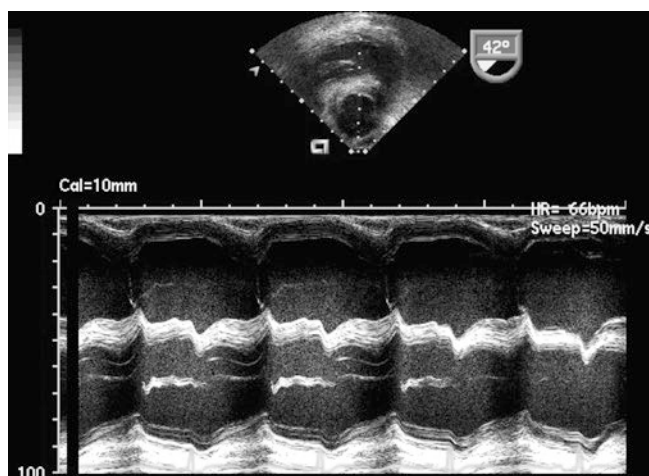
Fig. 5.17 M-mode echocardiogram obtained by transgastric imaging as shown in Video 5.3d. The paradoxical septal wall motion secondary to the right ventricular volume overload limits this method of quantitative assessment of ventricular function in this setting

Case 3

20 year old patient with history of tetralogy of Fallot and long-standing severe pulmonary regurgitation

Preoperative and postoperative TEE images are depicted in Videos 5.3a, 5.3b, 5.3c, 5.3d, and 5.3e. These views represent suitable imaging planes for qualitative interrogation of the ventricular functional abnormalities in this patient. The transgastric mid ventricular short axis view (Video 5.3d) is well suited for M-mode interrogation although, as shown in this case (Fig. 5.17), paradoxical septal motion may limit quantitative determination of LV systolic function.

References

1. Cyran SE, Kimball TR, Meyer RA, et al. Efficacy of intraoperative transesophageal echocardiography in children with congenital heart disease. Am J Cardiol. 1989;63:594–8.
2. Ritter SB. Transesophageal echocardiography in children: new peephole to the heart [comment]. J Am Coll Cardiol. 1990;16:447–50.
3. Stumper OF, Elzenga NJ, Hess J, Sutherland GR. Transesophageal echocardiography in children with congenital heart disease: an initial experience. J Am Coll Cardiol. 1990;16:433–41.
4. Ungerleider RM, Greeley WJ, Sheikh KH, et al. Routine use of intraoperative epicardial echocardiography and Doppler color flow imaging to guide and evaluate repair of congenital heart lesions. A prospective study. J Thorac Cardiovasc Surg. 1990; 100:297–309.
5. Fyfe DA, Kline CH, Sade RM, Greene CA, Gillette PC. The utility of transesophageal echocardiography during and after Fontan operations in small children. Am Heart J. 1991;122:1403–15.
6. Stevenson JG, Sorensen GK, Gartman DM, Hall DG, Rittenhouse EA. Transesophageal echocardiography during repair of congenital cardiac defects: identification of residual problems necessitating reoperation. J Am Soc Echocardiogr. 1993;6:356–65.
7. Stevenson JG. Role of intraoperative transesophageal echocardiography during repair of congenital cardiac defects. Acta Paediatr Suppl. 1995;410:23–33.
8. Ninomiya J, Yamauchi H, Hosaka H, et al. Continuous transoesophageal echocardiography monitoring during weaning from cardiopulmonary bypass in children. Cardiovasc Surg. 1997;5: 129–33.
9. Rice MJ, McDonald RW, Li X, Shen I, Ungerleider RM, Sahn DJ. New technology and methodologies for intraoperative, perioperative, and intraprocedural monitoring of surgical and catheter interventions for congenital heart disease. Echocardiography. 2002;19:725–34.
10. Stumper O, Witsenburg M, Sutherland GR, Cromme-Dijkhuis A, Godman MJ, Hess J. Transesophageal echocardiographic monitoring of interventional cardiac catheterization in children. J Am Coll Cardiol. 1991;18:1506–14.
11. Ludomirsky A. The use of echocardiography in pediatric interventional cardiac catheterization procedures. J Interv Cardiol. 1995;8:569–78.
12. Tumbarello R, Sanna A, Cardu G, Bande A, Napoleone A, Bini RM. Usefulness of transesophageal echocardiography in the pediatric catheterization laboratory. Am J Cardiol. 1993;71:1321–5.
13. Rigby ML. Transoesophageal echocardiography during interventional cardiac catheterisation in congenital heart disease. Heart. 2001;86 Suppl 2:II23–9.
14. Simon P, Mohl W. Intraoperative echocardiographic assessment of global and regional myocardial function. Echocardiography. 1990; 7:333–41.
15. Skiles JA, Griffin BP. Transesophageal echocardiographic (TEE) evaluation of ventricular function. Cardiol Clin. 2000;18:681–97, vii.
16. Schiller NB, Shah PM, Crawford M, et al. Recommendations for quantitation of the left ventricle by two-dimensional echocardiography. American Society of Echocardiography Committee on Standards, Subcommittee on Quantitation of Two-Dimensional Echocardiograms. J Am Soc Echocardiogr. 1989;2:358–67.
17. Abel MD, Nishimura RA, Callahan MJ, Rehder K, Ilstrup DM, Tajik AJ. Evaluation of intraoperative transesophageal two-dimensional echocardiography. Anesthesiology. 1987;66:64–8.
18. Nishimura RA, Abel MD, Housmans PR, Warnes CA, Tajik AJ. Mitral flow velocity curves as a function of different loading conditions: evaluation by intraoperative transesophageal Doppler echocardiography. J Am Soc Echocardiogr. 1989;2:79–87.
19. Kuecherer HF, Muhiudeen IA, Kusumoto FM, et al. Estimation of mean left atrial pressure from transesophageal pulsed Doppler echocardiography of pulmonary venous flow. Circulation. 1990;82: 1127–39.
20. Kuecherer HF, Kusumoto F, Muhiudeen IA, Cahalan MK, Schiller NB. Pulmonary venous flow patterns by transesophageal pulsed Doppler echocardiography: relation to parameters of left ventricular systolic and diastolic function. Am Heart J. 1991;122: 1683–93.
21. Muhiudeen IA, Kuecherer HF, Lee E, Cahalan MK, Schiller NB. Intraoperative estimation of cardiac output by transesophageal pulsed Doppler echocardiography. Anesthesiology. 1991;74:9–14.
22. Savino JS, Troianos CA, Aukburg S, Weiss R, Reichek N. Measurement of pulmonary blood flow with transesophageal two-dimensional and Doppler echocardiography. Anesthesiology. 1991;75:445–51.
23. Gorcsan 3rd J, Diana P, Ball BA, Hattler BG. Intraoperative determination of cardiac output by transesophageal continuous wave Doppler. Am Heart J. 1992;123:171–6.

24. Smith MD, MacPhail B, Harrison MR, Lenhoff SJ, DeMaria AN. Value and limitations of transesophageal echocardiography in determination of left ventricular volumes and ejection fraction. J Am Coll Cardiol. 1992;19:1213–22.

25. Stoddard MF, Dillon S, Peters G, Kupersmith J. Left ventricular ejection fraction is increased during transesophageal echocardiography in patients with impaired ventricular function. Am Heart J. 1992;123:1005–10.

26. Doerr HK, Quinones MA, Zoghbi WA. Accurate determination of left ventricular ejection fraction by transesophageal echocardiography with a nonvolumetric method. J Am Soc Echocardiogr. 1993;6:476–81.

27. Kuecherer HF, Foster E. Hemodynamics by transesophageal echocardiography. Cardiol Clin. 1993;11:475–87.

28. Rafferty T, Durkin M, Harris S, et al. Transesophageal two-dimensional echocardiographic analysis of right ventricular systolic performance indices during coronary artery bypass grafting. J Cardiothorac Vasc Anesth. 1993;7:160–6.

29. Sutton DC, Cahalan MK. Intraoperative assessment of left ventricular function with transesophageal echocardiography. Cardiol Clin. 1993;11:389–98.

30. Darmon PL, Hillel Z, Mogtader A, Mindich B, Thys D. Cardiac output by transesophageal echocardiography using continuous-wave Doppler across the aortic valve. Anesthesiology. 1994;80:796–805, discussion 25A.

31. Pu M, Griffin BP, Vandervoort PM, Leung DY, Cosgrove 3rd DM, Thomas JD. Intraoperative validation of mitral inflow determination by transesophageal echocardiography: comparison of single-plane, biplane and thermodilution techniques. J Am Coll Cardiol. 1995;26:1047–53.

32. Hozumi T, Yoshikawa J, Yoshida K, Akasaka T, Takagi T, Yamamuro A. Three-dimensional echocardiographic measurement of left ventricular volumes and ejection fraction using a multiplane transesophageal probe in patients. Am J Cardiol. 1996;78:1077–80.

33. Troianos CA, Porembka DT. Assessment of left ventricular function and hemodynamics with transesophageal echocardiography. Crit Care Clin. 1996;12:253–72.

34. Kuhl HP, Franke A, Frielingsdorf J, et al. Determination of left ventricular mass and circumferential wall thickness by three-dimensional reconstruction: in vitro validation of a new method that uses a multiplane transesophageal transducer. J Am Soc Echocardiogr. 1997;10:107–19.

35. Kuhl HP, Franke A, Janssens U, et al. Three-dimensional echocardiographic determination of left ventricular volumes and function by multiplane transesophageal transducer: dynamic in vitro validation and in vivo comparison with angiography and thermodilution. J Am Soc Echocardiogr. 1998;11:1113–24.

36. Ochiai Y, Morita S, Tanoue Y, Kawachi Y, Tominaga R, Yasui H. Use of transesophageal echocardiography for postoperative evaluation of right ventricular function. Ann Thorac Surg. 1999;67:146–52, discussion 153.

37. Poelaert J, Schmidt C, Van Aken H, Hinder F, Mollhoff T, Loick HM. A comparison of transoesophageal echocardiographic Doppler across the aortic valve and the thermodilution technique for estimating cardiac output. Anaesthesia. 1999;54:128–36.

38. Kubota H, Furuse A, Kotsuka Y, et al. Cardiac function evaluated by transesophageal echocardiography during cardiopulmonary bypass. Jpn J Thorac Cardiovasc Surg. 2000;48:261–6.

39. Schiller NB. Hemodynamics derived from transesophageal echocardiography (TEE). Cardiol Clin. 2000;18:699–709.

40. Simmons LA, Weidemann F, Sutherland GR, et al. Doppler tissue velocity, strain, and strain rate imaging with transesophageal echocardiography in the operating room: a feasibility study. J Am Soc Echocardiogr. 2002;15:768–76.

41. Swaminathan M, Phillips-Bute BG, Mathew JP. An assessment of two different methods of left ventricular ejection time measurement by transesophageal echocardiography. Anesth Analg. 2003;97:642–7.

42. Poelaert JI, Schupfer G. Hemodynamic monitoring utilizing transesophageal echocardiography: the relationships among pressure, flow, and function. Chest. 2005;127:379–90.

43. Chen C, Rodriguez L, Guerrero JL, et al. Noninvasive estimation of the instantaneous first derivative of left ventricular pressure using continuous-wave Doppler echocardiography. Circulation. 1991;83:2101–10.

44. Greim CA, Roewer N, Laux G, Schulte am Esch J. On-line estimation of left ventricular stroke volume using transoesophageal echocardiography and acoustic quantification. Br J Anaesth. 1996;77:365–9.

45. Rhodes J, Marx GR, Tardif JC, et al. Evaluation of ventricular dP/dt before and after open heart surgery using transesophageal echocardiography. Echocardiography. 1997;14:15–22.

46. Declerck C, Hillel Z, Shih H, Kuroda M, Connery CP, Thys DM. A comparison of left ventricular performance indices measured by transesophageal echocardiography with automated border detection. Anesthesiology. 1998;89:341–9.

47. Kotoh K, Watanabe G, Ueyama K, et al. On-line assessment of regional ventricular wall motion by transesophageal echocardiography with color kinesis during minimally invasive coronary artery bypass grafting. J Thorac Cardiovasc Surg. 1999;117:912–7.

48. Vermes E, Houel R, Simon M, Le Besnerais P, Loisance D. Doppler tissue imaging to predict myocardial recovery during mechanical circulatory support. Ann Thorac Surg. 2000;70:2149–51.

49. Skarvan K, Filipovic M, Wang J, Brett W, Seeberger M. Use of myocardial tissue Doppler imaging for intraoperative monitoring of left ventricular function. Br J Anaesth. 2003;91:473–80.

50. Skulstad H, Andersen K, Edvardsen T, et al. Detection of ischemia and new insight into left ventricular physiology by strain Doppler and tissue velocity imaging: assessment during coronary bypass operation of the beating heart. J Am Soc Echocardiogr. 2004;17:1225–33.

51. David JS, Tousignant CP, Bowry R. Tricuspid annular velocity in patients undergoing cardiac operation using transesophageal echocardiography. J Am Soc Echocardiogr. 2006;19:329–34.

52. Borow KM, Neumann A, Marcus RH, Sareli P, Lang RM. Effects of simultaneous alterations in preload and afterload on measurements of left ventricular contractility in patients with dilated cardiomyopathy: comparisons of ejection phase, isovolumetric and end-systolic force-velocity indexes. J Am Coll Cardiol. 1992;20:787–95.

53. Kimball TR, Daniels SR, Loggie JM, Khoury P, Meyer RA. Relation of left ventricular mass, preload, afterload and contractility in pediatric patients with essential hypertension. J Am Coll Cardiol. 1993;21:997–1001.

54. Rowland DG, Gutgesell HP. Noninvasive assessment of myocardial contractility, preload, and afterload in healthy newborn infants. Am J Cardiol. 1995;75:818–21.

55. Kjaergaard J, Snyder EM, Hassager C, Oh JK, Johnson BD. Impact of preload and afterload on global and regional right ventricular function and pressure: a quantitative echocardiography study. J Am Soc Echocardiogr. 2006;19:515–21.

56. Ozdemir K, Balci S, Duzenli MA, et al. Effect of preload and heart rate on the Doppler and tissue Doppler-derived myocardial performance index. Clin Cardiol. 2007;30:342–8.

57. Bailey JM, Shanewise JS, Kikura M, Sharma S. A comparison of transesophageal and transthoracic echocardiographic assessment of left ventricular function in pediatric patients with congenital heart disease. J Cardiothorac Vasc Anesth. 1995;9:665–9.

58. Silverman NH, Ports TA, Snider AR, Schiller NB, Carlsson E, Heilbron DC. Determination of left ventricular volume in children: echocardiographic and angiographic comparisons. Circulation. 1980;62:548–57.

59. Quinones MA, Waggoner AD, Reduto LA, et al. A new, simplified and accurate method for determining ejection fraction with two-dimensional echocardiography. Circulation. 1981;64:744–53.

60. Mercier JC, DiSessa TG, Jarmakani JM, et al. Two-dimensional echocardiographic assessment of left ventricular volumes and ejection fraction in children. Circulation. 1982;65:962–9.

61. Harrison MR, Clifton GD, Berk MR, DeMaria AN. Effect of blood pressure and afterload on Doppler echocardiographic measurements of left ventricular systolic function in normal subjects. Am J Cardiol. 1989;64:905–8.

62. Bashein G, Sheehan FH, Nessly ML, Detmer PR, Martin RW. Three-dimensional transesophageal echocardiography for depiction of regional left-ventricular performance: initial results and future directions. Int J Card Imaging. 1993;9:121–31.

63. Hozumi T, Yoshikawa J. Three-dimensional echocardiography using a multiplane transesophageal probe: the clinical applications. Echocardiography. 2000;17:757–64.

64. Mizelle KM, Rice MJ, Sahn DJ. Clinical use of real-time three-dimensional echocardiography in pediatric cardiology. Echocardiography. 2000;17:787–90.

65. Keller AM. Positional localization: three-dimensional transthoracic echocardiographic techniques for the measurement of cardiac mass, volume, and function. Echocardiography. 2000;17:745–8.

66. Azran MS, Kwong R, Chen FY, Shernan SK. A potential use for intraoperative three-dimensional transesophageal echocardiography in predicting left ventricular chamber dimensions and ejection fraction after aneurysm resection. Anesth Analg. 2010;111:1362–5.

67. Perez JE, Waggoner AD, Barzilai B, Melton HEJ, Miller JG, Sobel BE. On-line assessment of ventricular function by automatic boundary detection and ultrasonic backscatter imaging. J Am Coll Cardiol. 1992;19:313–20.

68. Gorcsan 3rd J, Romand JA, Mandarino WA, Deneault LG, Pinsky MR. Assessment of left ventricular performance by on-line pressure-area relations using echocardiographic automated border detection. J Am Coll Cardiol. 1994;23:242–52.

69. Gorcsan 3rd J, Denault A, Mandarino WA, Pinsky MR. Left ventricular pressure-volume relations with transesophageal echocardiographic automated border detection: comparison with conductance-catheter technique. Am Heart J. 1996;131:544–52.

70. Liu N, Darmon PL, Saada M, et al. Comparison between radionuclide ejection fraction and fractional area changes derived from transesophageal echocardiography using automated border detection. Anesthesiology. 1996;85:468–74.

71. Chandra S, Bahl VK, Reddy SC, Bhargava B, Malhotra A, Wasir HS. Comparison of echocardiographic acoustic quantification system and radionuclide ventriculography for estimating left ventricular ejection fraction: validation in patients without regional wall motion abnormalities. Am Heart J. 1997;133:359–63.

72. Denault AY, Gorcsan 3rd J, Mandarino WA, Kancel MJ, Pinsky MR. Left ventricular performance assessed by echocardiographic automated border detection and arterial pressure. Am J Physiol. 1997;272:H138–47.

73. Schmidlin D, Aschkenasy S, Vogt PR, Schmidli J, Jenni R, Schmid ER. Left ventricular pressure-area relations as assessed by transoesophageal echocardiographic automated border detection: comparison with conductance catheter technique in cardiac surgical patients. Br J Anaesth. 2000;85:379–88.

74. Tynan M, Reid DS, Hunter S, et al. Ejection phase indices of left ventricular performance in infants, children, and adults. Br Heart J. 1975;37:196–202.

75. Igarashi H, Shiraishi H, Endoh H, Yanagisawa M. Left ventricular contractile state in preterm infants: relation between wall stress and velocity of circumferential fiber shortening. Am Heart J. 1994;127:1336–40.

76. Fisher EA, DuBrow IW, Hastreiter AR. Comparison of ejection phase indices of left ventricular performance in infants and children. Circulation. 1975;52:916–25.

77. Gutgesell HP, Paquet M, Duff DF, McNamara DG. Evaluation of left ventricular size and function by echocardiography. Results in normal children. Circulation. 1977;56:457–62.

78. Henry WL, Ware J, Gardin JM, Hepner SI, McKay J, Weiner M. Echocardiographic measurements in normal subjects. Growth-related changes that occur between infancy and early adulthood. Circulation. 1978;57:278–85.

79. Ruschhaupt DG, Sodt PC, Hutcheon NA, Arcilla RA. Estimation of circumferential fiber shortening velocity by echocardiography. J Am Coll Cardiol. 1983;2:77–84.

80. Greim CA, Roewer N, Schulte am Esch J. Assessment of changes in left ventricular wall stress from the end-systolic pressure-area product. Br J Anaesth. 1995;75:583–7.

81. Colan SD, Borow KM, Neumann A. Left ventricular end-systolic wall stress-velocity of fiber shortening relation: a load-independent index of myocardial contractility. J Am Coll Cardiol. 1984;4:715–24.

82. Royse CF, Connelly KA, MacLaren G, Royse AG. Evaluation of echocardiography indices of systolic function: a comparative study using pressure-volume loops in patients undergoing coronary artery bypass surgery. Anaesthesia. 2007;62:109–16.

83. Tei C. New non-invasive index for combined systolic and diastolic ventricular function. J Cardiol. 1995;26:135–6.

84. Tei C, Ling LH, Hodge DO, et al. New index of combined systolic and diastolic myocardial performance: a simple and reproducible measure of cardiac function—a study in normals and dilated cardiomyopathy. J Cardiol. 1995;26:357–66.

85. Tei C, Dujardin KS, Hodge DO, Kyle RA, Tajik AJ, Seward JB. Doppler index combining systolic and diastolic myocardial performance: clinical value in cardiac amyloidosis. J Am Coll Cardiol. 1996;28:658–64.

86. Tei C, Nishimura RA, Seward JB, Tajik AJ. Noninvasive Doppler-derived myocardial performance index: correlation with simultaneous measurements of cardiac catheterization measurements. J Am Soc Echocardiogr. 1997;10:169–78.

87. Broberg CS, Pantely GA, Barber BJ, et al. Validation of the myocardial performance index by echocardiography in mice: a noninvasive measure of left ventricular function. J Am Soc Echocardiogr. 2003;16:814–23.

88. Eidem BW, Tei C, O'Leary PW, Cetta F, Seward JB. Nongeometric quantitative assessment of right and left ventricular function: myocardial performance index in normal children and patients with Ebstein anomaly. J Am Soc Echocardiogr. 1998;11:849–56.

89. Tei C, Dujardin KS, Hodge DO, et al. Doppler echocardiographic index for assessment of global right ventricular function. J Am Soc Echocardiogr. 1996;9:838–47.

90. Dujardin KS, Tei C, Yeo TC, Hodge DO, Rossi A, Seward JB. Prognostic value of a Doppler index combining systolic and diastolic performance in idiopathic-dilated cardiomyopathy. Am J Cardiol. 1998;82:1071–6.

91. Yeo TC, Dujardin KS, Tei C, Mahoney DW, McGoon MD, Seward JB. Value of a Doppler-derived index combining systolic and diastolic time intervals in predicting outcome in primary pulmonary hypertension. Am J Cardiol. 1998;81:1157–61.

92. Eidem BW, O'Leary PW, Tei C, Seward JB. Usefulness of the myocardial performance index for assessing right ventricular function in congenital heart disease. Am J Cardiol. 2000;86:654–8.

93. Williams RV, Ritter S, Tani LY, Pagoto LT, Minich LL. Quantitative assessment of ventricular function in children with single ventricles using the Doppler myocardial performance index. Am J Cardiol. 2000;86:1106–10.

94. Yasuoka K, Harada K, Toyono M, Tamura M, Yamamoto F. Tei index determined by tissue Doppler imaging in patients with pulmonary regurgitation after repair of tetralogy of Fallot. Pediatr Cardiol. 2004;25:131–6.

95. Shanewise JS, Cheung AT, Aronson S, et al. ASE/SCA guidelines for performing a comprehensive intraoperative multiplane

transesophageal echocardiography examination: recommendations of the American Society of Echocardiography Council for Intraoperative Echocardiography and the Society of Cardiovascular Anesthesiologists Task Force for Certification in Perioperative Transesophageal Echocardiography. J Am Soc Echocardiogr. 1999;12:884–900.

96. Cerqueira MD, Weissman NJ, Dilsizian V, et al. Standardized myocardial segmentation and nomenclature for tomographic imaging of the heart: a statement for healthcare professionals from the Cardiac Imaging Committee of the Council on Clinical Cardiology of the American Heart Association. Circulation. 2002;105:539–42.

97. Lang RM, Bierig M, Devereux RB, et al. Recommendations for chamber quantification: a report from the American Society of Echocardiography's Guidelines and Standards Committee and the Chamber Quantification Writing Group, developed in conjunction with the European Association of Echocardiography, a branch of the European Society of Cardiology. J Am Soc Echocardiogr. 2005;18:1440–63.

98. Rouine-Rapp K, Rouillard KP, Miller-Hance W, et al. Segmental wall-motion abnormalities after an arterial switch operation indicate ischemia. Anesth Analg. 2006;103:1139–46.

99. Eidem BW, McMahon CJ, Cohen RR, et al. Impact of cardiac growth on Doppler tissue imaging velocities: a study in healthy children. J Am Soc Echocardiogr. 2004;17:212–21.

100. McMahon CJ, Nagueh SF, Pignatelli RH, et al. Characterization of left ventricular diastolic function by tissue Doppler imaging and clinical status in children with hypertrophic cardiomyopathy. Circulation. 2004;109:1756–62.

101. Nagueh SF, Middleton KJ, Kopelen HA, Zoghbi WA, Quinones MA. Doppler tissue imaging: a noninvasive technique for evaluation of left ventricular relaxation and estimation of filling pressures. J Am Coll Cardiol. 1997;30:1527–33.

102. Nagueh SF, Mikati I, Kopelen HA, Middleton KJ, Quinones MA, Zoghbi WA. Doppler estimation of left ventricular filling pressure in sinus tachycardia. A new application of tissue Doppler imaging. Circulation. 1998;98:1644–50.

103. Sasaki N, Garcia M, Lytrivi I, et al. Utility of Doppler tissue imaging-derived indices in identifying subclinical systolic ventricular dysfunction in children with restrictive cardiomyopathy. Pediatr Cardiol. 2011;32:646–51.

104. Goldberg DJ, Quartermain MD, Glatz AC, et al. Doppler tissue imaging in children following cardiac transplantation: a comparison to catheter derived hemodynamics. Pediatr Transplant. 2011;15:488–94.

105. Derumeaux G, Ovize M, Loufoua J, Pontier G, Andre-Fouet X, Cribier A. Assessment of nonuniformity of transmural myocardial velocities by color-coded tissue Doppler imaging: characterization of normal, ischemic, and stunned myocardium. Circulation. 2000;101:1390–5.

106. Weidemann F, Eyskens B, Jamal F, et al. Quantification of regional left and right ventricular radial and longitudinal function in healthy children using ultrasound-based strain rate and strain imaging. J Am Soc Echocardiogr. 2002;15:20–8.

107. Weidemann F, Eyskens B, Mertens L, et al. Quantification of regional right and left ventricular function by ultrasonic strain rate and strain indexes after surgical repair of tetralogy of Fallot. Am J Cardiol. 2002;90:133–8.

108. Harada K, Toyono M, Yamamoto F. Assessment of right ventricular function during exercise with quantitative Doppler tissue imaging in children late after repair of tetralogy of Fallot. J Am Soc Echocardiogr. 2004;17:863–9.

109. Toyono M, Harada K, Tamura M, Yamamoto F, Takada G. Myocardial acceleration during isovolumic contraction as a new index of right ventricular contractile function and its relation to pulmonary regurgitation in patients after repair of tetralogy of Fallot. J Am Soc Echocardiogr. 2004;17:332–7.

110. Eyskens B, Ganame J, Taylor AM, et al. Reduced right ventricular deformation in children with severe pulmonary regurgitation after tetralogy of Fallot correction is associated with reduced exercise capacity. Circulation. 2005;112:17.

111. Friedberg MK, Mertens L. Tissue velocities, strain, and strain rate for echocardiographic assessment of ventricular function in congenital heart disease. Eur J Echocardiogr. 2009;10:585–93.

112. Nagueh SF, Appleton CP, Gillebert TC, et al. Recommendations for the evaluation of left ventricular diastolic function by echocardiography. J Am Soc Echocardiogr. 2009;22:107–33.

113. O'Leary PW, Durongpisitkul K, Cordes TM, et al. Diastolic ventricular function in children: a Doppler echocardiographic study establishing normal values and predictors of increased ventricular end-diastolic pressure. Mayo Clin Proc. 1998;73:616–28.

114. Olivier M, O'leary PW, Pankratz VS, et al. Serial Doppler assessment of diastolic function before and after the Fontan operation. J Am Soc Echocardiogr. 2003;16:1136–43.

115. Appleton CP, Hatle LK, Popp RL. Relation of transmitral flow velocity patterns to left ventricular diastolic function: new insights from a combined hemodynamic and Doppler echocardiographic study. J Am Coll Cardiol. 1988;12:426–40.

116. Nishimura RA, Abel MD, Hatle LK, Tajik AJ. Assessment of diastolic function of the heart: background and current applications of Doppler echocardiography. Part II. Clinical studies. Mayo Clin Proc. 1989;64:181–204.

117. Bessen M, Gardin JM. Evaluation of left ventricular diastolic function. Cardiol Clin. 1990;8:315–32.

118. Myreng Y, Smiseth OA. Assessment of left ventricular relaxation by Doppler echocardiography. Comparison of isovolumic relaxation time and transmitral flow velocities with time constant of isovolumic relaxation. Circulation. 1990;81:260–6.

119. Klein AL, Tajik AJ. Doppler assessment of pulmonary venous flow in healthy subjects and in patients with heart disease. J Am Soc Echocardiogr. 1991;4:379–92.

120. Appleton CP, Galloway JM, Gonzalez MS, Gaballa M, Basnight MA. Estimation of left ventricular filling pressures using two-dimensional and Doppler echocardiography in adult patients with cardiac disease. Additional value of analyzing left atrial size, left atrial ejection fraction and the difference in duration of pulmonary venous and mitral flow velocity at atrial contraction. J Am Coll Cardiol. 1993;22:1972–82.

121. Cohen GI, Pietrolungo JF, Thomas JD, Klein AL. A practical guide to assessment of ventricular diastolic function using Doppler echocardiography. J Am Coll Cardiol. 1996;27:1753–60.

122. Hoit BD, Shao Y, Gabel M, Walsh RA. Influence of loading conditions and contractile state on pulmonary venous flow. Validation of Doppler velocimetry. Circulation. 1992;86:651–9.

123. Sohn DW, Chai IH, Lee DJ, et al. Assessment of mitral annulus velocity by Doppler tissue imaging in the evaluation of left ventricular diastolic function. J Am Coll Cardiol. 1997;30:474–80.

124. Aranda JMJ, Weston MW, Puleo JA, Fontanet HL. Effect of loading conditions on myocardial relaxation velocities determined by Doppler tissue imaging in heart transplant recipients. J Heart Lung Transplant. 1998;17:693–7.

125. Oki T, Fukuda K, Tabata T, et al. Effect of an acute increase in afterload on left ventricular regional wall motion velocity in healthy subjects. J Am Soc Echocardiogr. 1999;12:476–83.

126. Muller S, Bartel T, Koopman J, Pandian NG, Erbel R, Pachinger O. Tissue Doppler analysis is hindered in abnormal wall motion and changes in afterload. Int J Cardiol. 2003;90:81–90.

127. Jacques DC, Pinsky MR, Severyn D, Gorcsan 3rd J. Influence of alterations in loading on mitral annular velocity by tissue Doppler echocardiography and its associated ability to predict filling pressures. Chest. 2004;126:1910–8.

128. Farias CA, Rodriguez L, Garcia MJ, Sun JP, Klein AL, Thomas JD. Assessment of diastolic function by tissue Doppler echocar-

diography: comparison with standard transmitral and pulmonary venous flow. J Am Soc Echocardiogr. 1999;12:609–17.

129. Garcia MJ, Thomas JD. Tissue Doppler to assess diastolic left ventricular function. Echocardiography. 1999;16:501–8.

130. Rivas-Gotz C, Khoury DS, Manolios M, Rao L, Kopelen HA, Nagueh SF. Time interval between onset of mitral inflow and onset of early diastolic velocity by tissue Doppler: a novel index of left ventricular relaxation: experimental studies and clinical application. J Am Coll Cardiol. 2003;42:1463–70.

131. Ruan Q, Rao L, Middleton KJ, Khoury DS, Nagueh SF. Assessment of left ventricular diastolic function by early diastolic mitral annulus peak acceleration rate: experimental studies and clinical application. J Appl Physiol. 2006;100:679–84.

132. Garcia MJ, Rodriguez L, Ares M, Griffin BP, Thomas JD, Klein AL. Differentiation of constrictive pericarditis from restrictive cardiomyopathy: assessment of left ventricular diastolic velocities in longitudinal axis by Doppler tissue imaging. J Am Coll Cardiol. 1996;27:108–14.

133. Oki T, Tabata T, Yamada H, et al. Right and left ventricular wall motion velocities as diagnostic indicators of constrictive pericarditis. Am J Cardiol. 1998;81:465–70.

134. Ha JW, Oh JK, Ommen SR, Ling LH, Tajik AJ. Diagnostic value of mitral annular velocity for constrictive pericarditis in the absence of respiratory variation in mitral inflow velocity. J Am Soc Echocardiogr. 2002;15:1468–71.

135. Ha JW, Ommen SR, Tajik AJ, et al. Differentiation of constrictive pericarditis from restrictive cardiomyopathy using mitral annular velocity by tissue Doppler echocardiography. Am J Cardiol. 2004;94:316–9.

136. Rychik J, Tian ZY. Quantitative assessment of myocardial tissue velocities in normal children with Doppler tissue imaging. Am J Cardiol. 1996;77:1254–7.

137. Harada K, Orino T, Yasuoka K, Tamura M, Takada G. Tissue Doppler imaging of left and right ventricles in normal children. Tohoku J Exp Med. 2000;191:21–9.

138. Kapusta L, Thijssen JM, Cuypers MH, Peer PG, Daniels O. Assessment of myocardial velocities in healthy children using tissue Doppler imaging. Ultrasound Med Biol. 2000;26:229–37.

139. Mori K, Hayabuchi Y, Kuroda Y, Nii M, Manabe T. Left ventricular wall motion velocities in healthy children measured by pulsed wave Doppler tissue echocardiography: normal values and relation to age and heart rate. J Am Soc Echocardiogr. 2000;13:1002–11.

140. Frommelt PC, Ballweg JA, Whitstone BN, Frommelt MA. Usefulness of Doppler tissue imaging analysis of tricuspid annular motion for determination of right ventricular function in normal infants and children. Am J Cardiol. 2002;89:610–3.

141. Swaminathan S, Ferrer PL, Wolff GS, Gomez-Marin O, Rusconi PG. Usefulness of tissue Doppler echocardiography for evaluating ventricular function in children without heart disease. Am J Cardiol. 2003;91:570–4.

142. Savage A, Hlavacek A, Ringewald J, Shirali G. Evaluation of the myocardial performance index and tissue Doppler imaging by comparison to near-simultaneous catheter measurements in pediatric cardiac transplant patients. J Heart Lung Transplant. 2010;29:853–8.

143. Nagueh SF, Kopelen HA, Quinones MA. Assessment of left ventricular filling pressures by Doppler in the presence of atrial fibrillation. Circulation. 1996;94:2138–45.

144. Sundereswaran L, Nagueh SF, Vardan S, et al. Estimation of left and right ventricular filling pressures after heart transplantation by tissue Doppler imaging. Am J Cardiol. 1998;82:352–7.

145. Nagueh SF, Lakkis NM, Middleton KJ, Spencer 3rd WH, Zoghbi WA, Quinones MA. Doppler estimation of left ventricular filling pressures in patients with hypertrophic cardiomyopathy. Circulation. 1999;99:254–61.

146. Border WL, Michelfelder EC, Glascock BJ, et al. Color M-mode and Doppler tissue evaluation of diastolic function in children:

simultaneous correlation with invasive indices. J Am Soc Echocardiogr. 2003;16:988–94.

147. Yock PG, Popp RL. Noninvasive estimation of right ventricular systolic pressure by Doppler ultrasound in patients with tricuspid regurgitation. Circulation. 1984;70:657–62.

148. Zoghbi WA, Habib GB, Quinones MA. Doppler assessment of right ventricular filling in a normal population. Comparison with left ventricular filling dynamics. Circulation. 1990;82:1316–24.

149. Moller JE, Poulsen SH, Egstrup K. Effect of preload alternations on a new Doppler echocardiographic index of combined systolic and diastolic performance. J Am Soc Echocardiogr. 1999;12:1065–72.

150. Poelaert J, Ruggero A. Myocardial performance index and tissue Doppler systolic wave velocity are preload dependent. Anesthesiology. 2005;103:210; author reply 210; author reply 211.

151. Anconina J, Danchin N, Selton-Suty C, et al. Noninvasive estimation of right ventricular dP/dt in patients with tricuspid valve regurgitation. Am J Cardiol. 1993;71:1495–7.

152. Pai RG, Bansal RC, Shah PM. Determinants of the rate of right ventricular pressure rise by Doppler echocardiography: potential value in the assessment of right ventricular function. J Heart Valve Dis. 1994;3:179–84.

153. Michelfelder EC, Vermilion RP, Ludomirsky A, Beekman RH, Lloyd TR. Comparison of simultaneous Doppler- and catheter-derived right ventricular dP/dt in hypoplastic left heart syndrome. Am J Cardiol. 1996;77:212–4.

154. Kanzaki H, Nakatani S, Kawada T, Yamagishi M, Sunagawa K, Miyatake K. Right ventricular dP/dt/P(max), not dP/dt(max), noninvasively derived from tricuspid regurgitation velocity is a useful index of right ventricular contractility. J Am Soc Echocardiogr. 2002;15:136–42.

155. Noori NM, Mehralizadeh S, Khaje A. Assessment of right ventricular function in children with congenital heart disease. Doppler tissue imaging. Saudi Med J. 2008;29:1168–72.

156. Helbing WA, Bosch HG, Maliepaard C, et al. On-line automated border detection for echocardiographic quantification of right ventricular size and function in children. Pediatr Cardiol. 1997;18:261–9.

157. Geva T, Powell AJ, Crawford EC, Chung T, Colan SD. Evaluation of regional differences in right ventricular systolic function by acoustic quantification echocardiography and cine magnetic resonance imaging. Circulation. 1998;98:339–45.

158. Jiang L, Siu SC, Handschumacher MD, et al. Three-dimensional echocardiography. In vivo validation for right ventricular volume and function. Circulation. 1994;89:2342–50.

159. Fujimoto S, Mizuno R, Nakagawa Y, Dohi K, Nakano H. Estimation of the right ventricular volume and ejection fraction by transthoracic three-dimensional echocardiography. A validation study using magnetic resonance imaging. Int J Card Imaging. 1998;14:385–90.

160. Ota T, Fleishman CE, Strub M, et al. Real-time, three-dimensional echocardiography: feasibility of dynamic right ventricular volume measurement with saline contrast. Am Heart J. 1999;137:958–66.

161. Grison A, Maschietto N, Reffo E, et al. Three-dimensional echocardiographic evaluation of right ventricular volume and function in pediatric patients: validation of the technique. J Am Soc Echocardiogr. 2007;20:921–9.

162. Tamborini G, Brusoni D, Torres Molina JE, et al. Feasibility of a new generation three-dimensional echocardiography for right ventricular volumetric and functional measurements. Am J Cardiol. 2008;102:499–505.

163. Tamborini G, Muratori M, Brusoni D, et al. Is right ventricular systolic function reduced after cardiac surgery? A two- and three-dimensional echocardiographic study. Eur J Echocardiogr. 2009;10:630–4.

164. Vegas A, Meineri M. Core review: three-dimensional transesophageal echocardiography is a major advance for intraoperative

clinical management of patients undergoing cardiac surgery: a core review. Anesth Analg. 2010;110:1548–73.

165. Cheung YF, Penny DJ, Redington AN. Serial assessment of left ventricular diastolic function after Fontan procedure. Heart. 2000;83:420–4.

166. Mahle WT, Coon PD, Wernovsky G, Rychik J. Quantitative echocardiographic assessment of the performance of the functionally single right ventricle after the Fontan operation. Cardiol Young. 2001;11:399–406.

167. Earing MG, Cetta F, Driscoll DJ, et al. Long-term results of the Fontan operation for double-inlet left ventricle. Am J Cardiol. 2005;96:291–8.

168. Frommelt PC, Snider AR, Meliones JN, Vermilion RP. Doppler assessment of pulmonary artery flow patterns and ventricu-

lar function after the Fontan operation. Am J Cardiol. 1991;68: 1211–5.

169. Penny DJ, Rigby ML, Redington AN. Abnormal patterns of intraventricular flow and diastolic filling after the Fontan operation: evidence for incoordinate ventricular wall motion. Br Heart J. 1991;66:375–8.

170. Bassareo PP, Tumbarello R, Piras A, Mercuro G. Evaluation of regional myocardial function by Doppler tissue imaging in univentricular heart after successful Fontan repair. Echocardiography. 2010;27:702–8.

171. Ikemba CM, Su JT, Stayer SA, et al. Myocardial performance index with sevoflurane-pancuronium versus fentanyl-midazolam-pancuronium in infants with a functional single ventricle. Anesthesiology. 2004;101:1298–305.